Available online at www.sciencedirect.com
ScienceDirect
Gondwana Research 10 (2006) 232–255
www.elsevier.com/locate/gr

Crustal architecture of the Himalayan metamorphic front in eastern Nepal

Ben Goscombe [a,*], David Gray [b], Martin Hand [a]

[a] Continental Evolution Research Group, School of Earth and Environmental Sciences, University of Adelaide, Adelaide, South Australia, 5005, Australia
[b] School of Earth Sciences, University of Melbourne, Melbourne, Victoria, 3010, Australia

Received 7 December 2005; received in revised form 5 May 2006; accepted 5 May 2006
Available online 18 September 2006

Abstract

The Himalayan Metamorphic Front consists of two basinal sequences deposited on the Indian passive margin, the Mesoproterozoic Lesser Himalayan Sequence and the Neoproterozoic–Cambrian Greater Himalayan Sequence. The current paradigm is that the unconformity between these two basinal sequences coincides with a crustal-scale thrust that has been called the Main Central Thrust, and that this acted as the fundamental structure that controlled the architecture of the Himalayan Metamorphic Front. Geological mapping of eastern Nepal and eight detailed stratigraphic, kinematic, strain and metamorphic profiles through the Himalayan Metamorphic Front define the crustal architecture. In eastern Nepal the unconformity does not coincide with a discrete structural or metamorphic discontinuity and is not a discrete high strain zone. In recognition of this, we introduce the term Himalayan Unconformity to distinguish it from high strain zones in the Himalayan Metamorphic Front. The fundamental structure that controls orogen architecture in eastern Nepal occurs at higher structural levels within the Greater Himalayan Sequence and we suggest the name; High Himal Thrust. This 100–400 m thick mylonite zone marks a sharp deformation discontinuity associated with a steep metamorphic transition, and separates the Upper-Plate from the Lower-Plate in the Himalayan Metamorphic Front. The high-*T*/moderate-*P* metamorphism at ~20–24 Ma in the Upper-Plate reflects extrusion of material between the High Himal Thrust and the South Tibet Detachment System at the top of the section. The Lower-Plate is a broad schistose zone of inverted, diachronous moderate-*T*/high-*P* metamorphic rocks formed between ~18 and 6 Ma. The High Himal Thrust is laterally continuous into Sikkim and Bhutan where it also occurs at higher structural levels than the Himalayan Unconformity and Main Central Thrust (as originally defined). To the west in central Nepal, the Upper-Plate/Lower-Plate boundary has been placed at lower structural levels, coinciding with the Himalayan Unconformity and has been named the Main Central Thrust, above the originally defined Main Central Thrust (or Ramgarh Thrust).

Keywords: Himalayan tectonics; Orogen architecture; Metamorphic field gradients; Strain field gradients; Kinematics; Crustal shear zones

1. Introduction

The tectonics of the Himalayan Orogen (Fig. 1) has been the focus of enormous attention over the last 20 years because it is both an active collisional orogen and the quintessential example of high-angle convergence. The structural and metamorphic architecture however, is not equally well known in all parts of the Himalayan Orogen, particularly the eastern Nepal region (Fig. 2) that links the well-investigated regions of the central Himalaya: central Nepal (e.g. Inger and Harris, 1992; Hodges et al., 1996; Hubbard, 1996; Vannay and Hodges, 1996; Harrison et al., 1997; Kohn et al., 2001, 2005), and Sikkim–Bhutan (e.g. Davidson et al., 1997; Grujic et al., 1996; Daniel et al., 2003; Catlos et al., 2004; Dasgupta et al., 2004; Harris et al., 2004; Searle and Szulc, 2005). In this paper we describe the crustal architecture of the Himalayan Metamorphic Front in eastern Nepal between Mount Everest and Kangchenjunga, by utilizing 8 detailed profiles that document stratigraphic rock units, crustal-scale structures, strain, kinematics and metamorphic zonation (Fig. 3).

The problem has been that the Main Central Thrust (MCT), a structural feature, has in part been correlated with a stratigraphic unconformity and interpreted to occur at multiple structural levels in some regions, with these structural positions varying along the orogen (Fig. 4; see Regional geology). As a result, there is a level of ambiguity pertaining to both nomenclature and relative importance of structures within the Himalayan Metamorphic Front; and ultimately also to the crustal architecture. In this paper we address these issues from a field-based description of the eastern Nepal portion of the orogenic front.

* Corresponding author.
E-mail address: ben.goscombe@adelaide.edu.au (B. Goscombe).

1342-937X/$ - see front matter © 2006 International Association for Gondwana Research. Published by Elsevier B.V. All rights reserved.
doi:10.1016/j.gr.2006.05.003

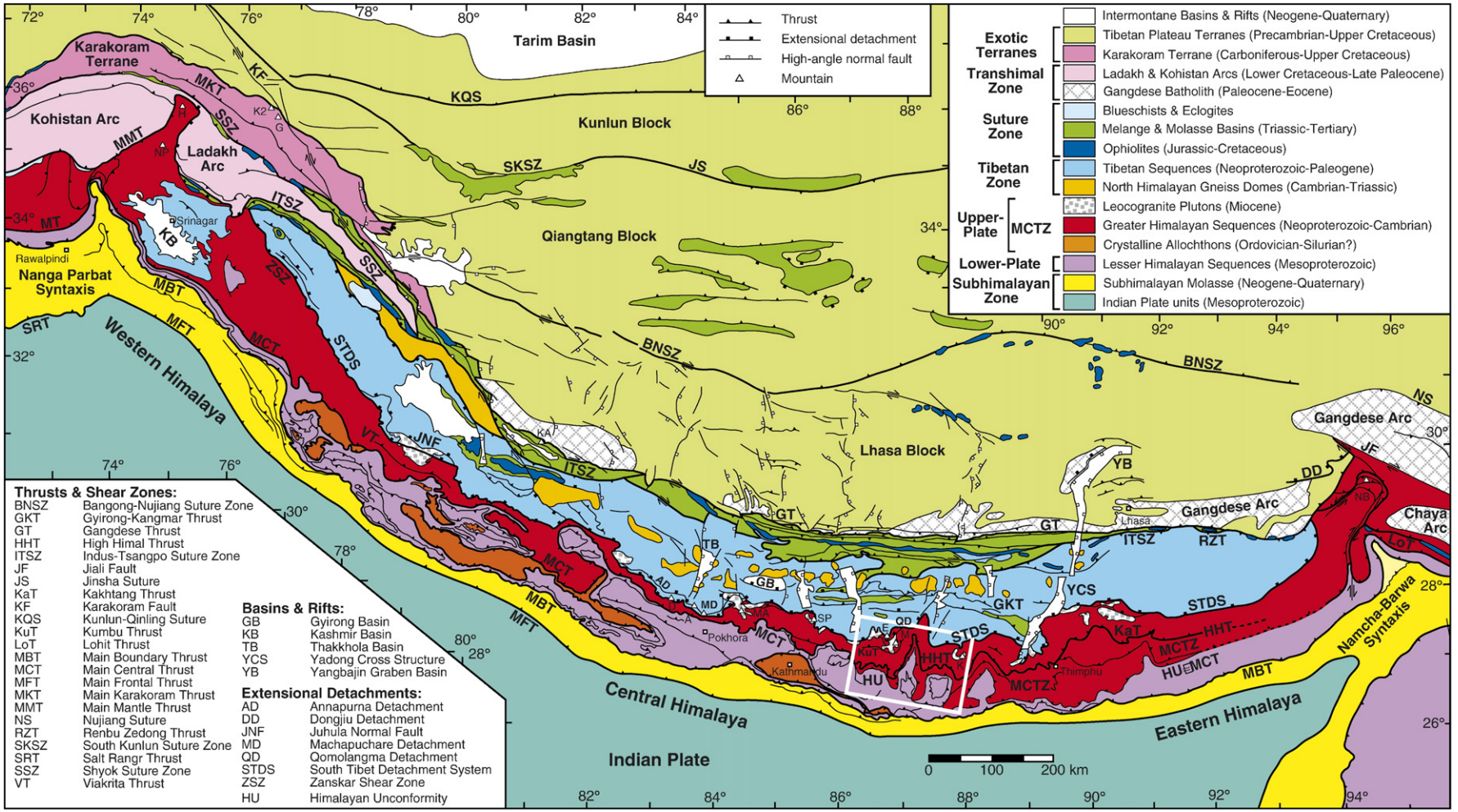

Fig. 1. Simplified geology of the Himalayan Orogen, showing main tectonostratigraphic rock units and major structures. Based on a compilation of >50 publications and the authors mapping in the eastern Nepal study area (Fig. 6) outlined by a white box.

2. Regional geology

The greater, 2500 km by 1000 km, Pamir-Himalaya-Tibet Orogen (Fig. 1) has experienced a protracted history from ~250 Ma, involving initial growth by subduction accretion and arc/terrane docking along the southern margin of the Asian Plate (Fig. 5; Schwab et al., 2004 and references cited therein). This was concluded by closure of the Neotethys Ocean at the Indus-Yarlung-Tsangpo Suture and collision between the Asian and Indo-Australian Plates from ~55 to 50 Ma (Tapponier et al., 1982; Patriat and Achache, 1984; Tapponier et al., 1986; Dewey et al., 1989; LePichon et al., 1992; Zhu et al., 2005; Leech et al., 2005). Collision brought basinal sequences deposited on the Indian Plate passive margin against the Neoproterozoic to Eocene Tethyan Sequence, at ~35–30 Ma, along the Eohimalayan Thrust (Fig. 5; Vannay and Hodges, 1996; Godin et al., 2001) that was later reactivated as the South Tibet Detachment System (STDS). Subsequent to collision, shallow, north-dipping thrusts systems became progressively activated and the main orogenic front migrated southward from the Trans-Himalaya to central Himalaya (Fig. 5; Hodges, 2000 and references cited therein). The current orogenic front of intensely deformed metamorphic rocks, between the STDS and the Main Boundary Thrust, is the focus of this paper and has been called the Himalayan Metamorphic Front (e.g. Goscombe et al., 2003).

Within the Himalayan Metamorphic Front two laterally continuous basinal sequences have been pervasively deformed and metamorphosed (LeFort, 1975). Both were deposited on the Indian Plate and are not separated by a suture or other crustal-scale structure. At the lowest structural level is the Palaeo- to Mesoproterozoic Lesser Himalayan Sequence overlain by Neoproterozoic to Cambrian Greater Himalayan Sequence (Parrish and Hodges, 1996; Upreti, 1999; Hodges, 2000; DeCelle et al., 2000; Robinson et al., 2001). Both sequences have unique provenance; the Lesser Himalayan Sequence has $\varepsilon_{Nd}(0)$ values ranging −20 to −26 and the Greater Himalayan Sequence ranges from −11 to −18 (Parrish and Hodges, 1996; Ahmad et al., 2000; Robinson et al., 2001; Martin et al., 2005 and references cited therein). Previously, the unconformity between these two basinal sequences has been mapped as a structural contact and incorrectly referred to as the Main Central Thrust (MCT) as discussed below. It has also been noted that the unconformity commonly coincides with the kyanite-in isograd (e.g. LeFort, 1975; Pêcher, 1989; Kohn et al., 2001; Upreti and Yoshida, 2005). Within the Himalayan Metamorphic Front, detailed positioning of the unconformity on lithostratigraphic grounds (Colchen et al., 1986) and Nd isotopic mapping, has shown that the unconformity does not necessarily coincide with a discrete thrust (Fig. 4; Searle et al., 2002). The unconformity needs to be defined independently of strain and metamorphism, and we propose the term Himalayan Unconformity, to distinguish the stratigraphic unconformity from the deformational MCT (Figs. 3 and 4; Goscombe et al., 2003).

Superimposed on the stratigraphic units in the Himalayan Metamorphic Front is a high strain crustal-scale thrust that marks a deformational-metamorphic-chronologic discontinuity

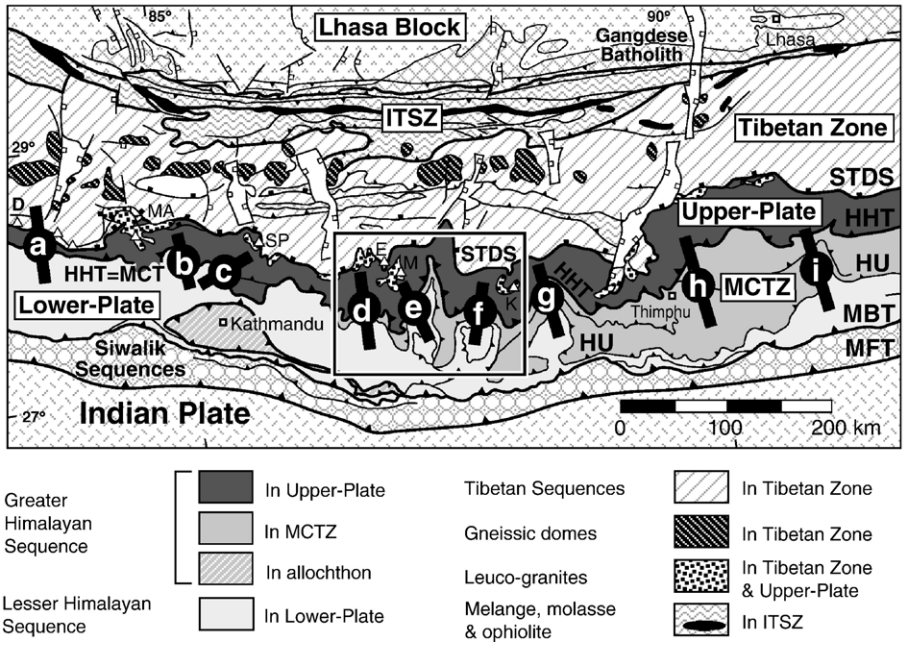

Fig. 2. Simplified tectonic map of the central Himalayan Orogen. The location of structural and metamorphic profiles referred to from the literature are indicated: (a) Dhaulagiri and Annapurna Himals, (b) Mahesh and Darondi valleys, (c) Langtang valley, (d) Kumbu Himal, (e) Arun River profiles, (f) Tamor and Yangma Rivers, (g) Sikkim profiles and (h) western and (i) eastern Bhutan profiles. The portion of the Himalayan Metamorphic Front investigated in this study covers profiles (d) to (f). Abbreviations of major crustal structures: STDS—South Tibet Detachment System, HHT—High Himal Thrust, HU—Himalayan Unconformity, MCT—Main Central Thrusts (coincident with HHT in the west and to the east is close to the Himalayan Unconformity as originally defined; Fig. 4), MCTZ—Main Central Thrust Zone of pervasive shear and inverted metamorphism between the Himalayan Unconformity and HHT, MBT—Main Boundary Thrust, MFT—Main Frontal Thrust, ITSZ—Indus-Tsangpo Suture Zone. Major mountains indicated by triangles with the following abbreviations: D—Dhaulagiri, MA—Manaslu, SP—Shisha Pangma, E—Everest, M—Makalu, K—Kangchenjunga.

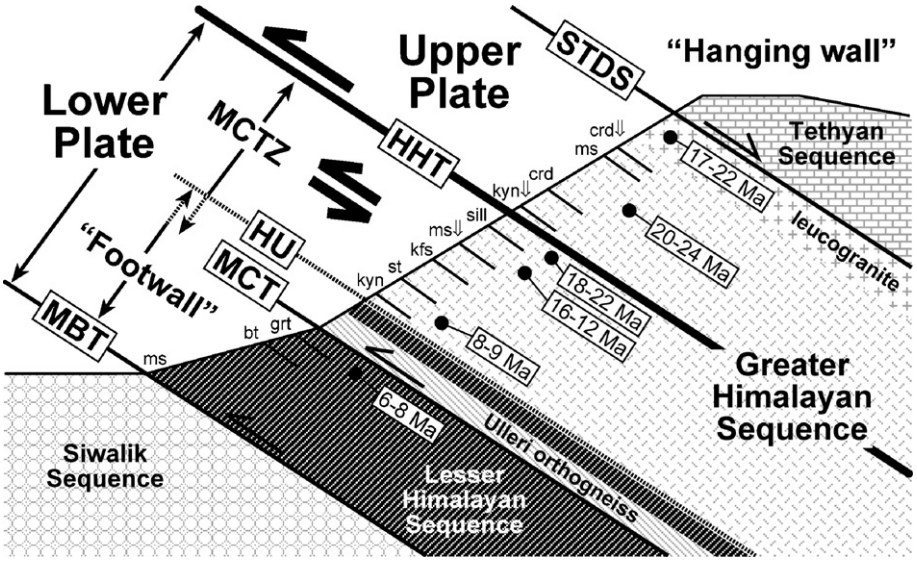

Fig. 3. Summary of nomenclature, stratigraphy, crustal architecture and mineral isograds in eastern Nepal. U–Pb–Th monazite age determinations (Ma) from Nepal, Sikkim and Bhutan are summarized in boxes (Harrison et al., 1997, 1999; Simpson et al., 2000; Kohn et al., 2001; Daniel et al., 2003; Catlos et al., 2004; Kohn et al., 2005). Abbreviations defined in Fig. 2.

that is responsible for an Upper-Plate/Lower-Plate architecture. This discontinuity separates the high-grade rocks of the Higher Himalayan Zone (also called Tibetan Slab or High Himalayan Crystallines) from the high-strain inverted amphibolite facies rocks in the Main Central Thrust Zone (MCTZ) and lower grade footwall rocks of the Lesser Himalayan Zone (e.g. Hodges, 2000; Hodges et al., 2001). The Upper-Plate is the thick high-grade slab that extruded southward over the Lower-Plate inverted metamorphic rocks (e.g. Grujic et al., 1996; Hodges et al., 2001; Beaumont et al., 2001). The fundamental Upper-Plate/Lower-Plate boundary occurs within the Greater Himalayan Sequence, at a structural level higher than the Himalayan Unconformity in eastern Nepal (Figs. 3 and 6) and possibly also central Nepal (Searle et al., 2002; Figs. 2 and 4). In contrast,

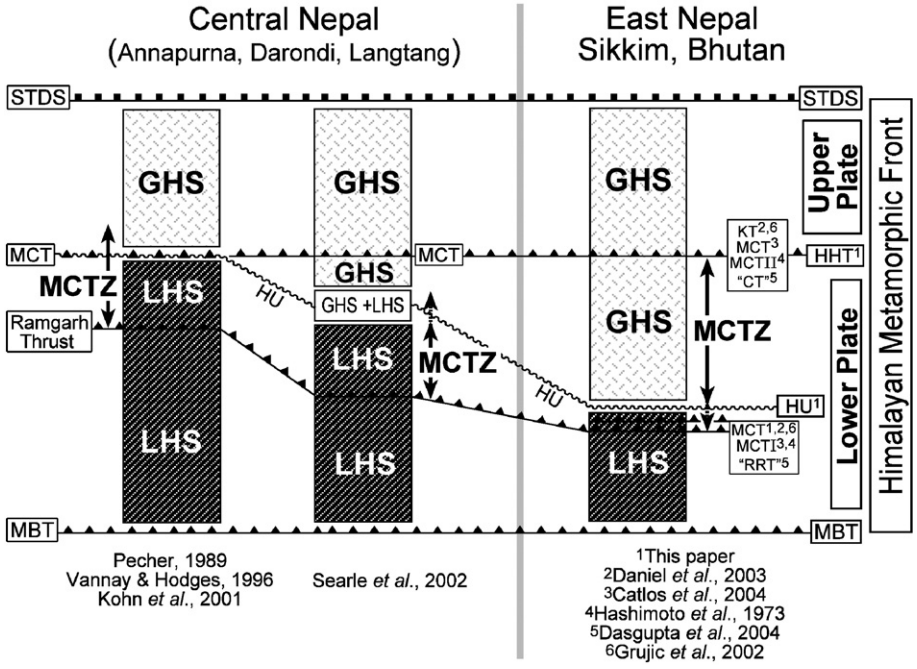

Fig. 4. Summary of relationships between stratigraphic units and named crustal structures that differ between the central Nepal region (profiles a to c in Fig. 2) and regions to the east including those investigated in this study (profiles d to i). The column and nomenclature on the far right (east) are those used in this paper (Fig. 3) and interpreted to be applicable into Sikkim (Fig. 2 in Dasgupta et al., 2004) and Bhutan (Grujic et al., 2002; Daniel et al., 2003). The numbered references refer to alternative names of structures used by the respective authors. Abbreviations are defined in Fig. 2 and also; "RRT"—thrust through Rangpo-Rangit and "CT"—thrust through Chungthang in Sikkim, KT—Kakhtang Thrust in Bhutan, GHS—Greater Himalayan Sequence and LHS—Lesser Himalayan Sequence.

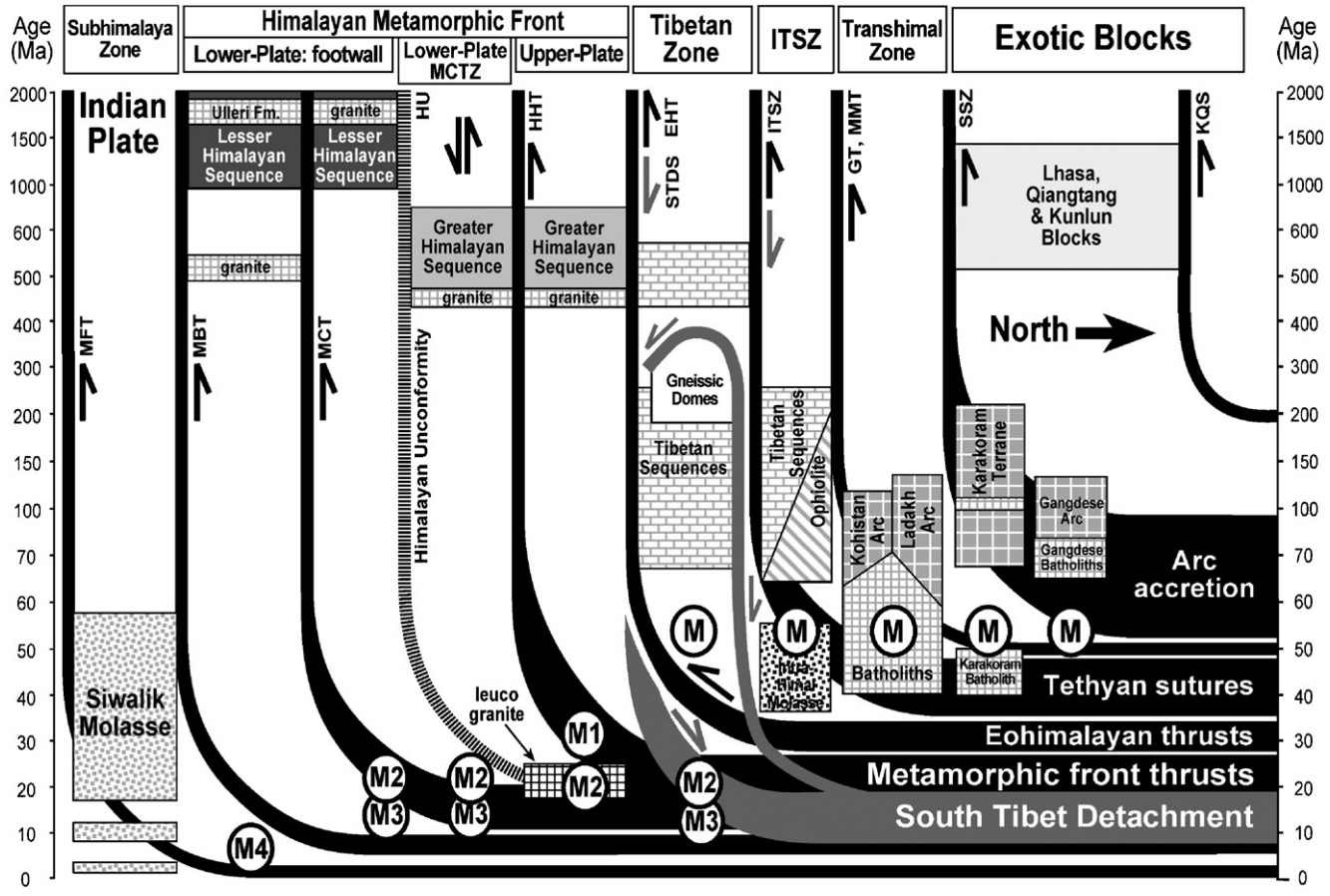

Fig. 5. Time-space diagram across the central Himalayan–Tibetan Orogen. The main tectonostratigraphic rock units are arranged along the horizontal axis from south to north towards the right. Time progresses down the page along a non-linear scale in Ma. Age range of rock units are indicated by boxes. Major crustal structures (solid thick lines) are positioned with respect to the terranes and rock units that they bound. Duration of deformation in each structure indicated by line width against vertical, right hand axis. STDS and ITSZ have been reactivated at different times by opposing transport. Early reverse movement at the Eohimalayan Thrust (EHT) preceded the STDS. The unconformity between the Lesser- and Greater Himalayan Sequences has been variably reworked and is shown by a dashed line. Successive metamorphic events recognised in the Himalayan Metamorphic Front are indicated in circles: M1—~30–35 Ma, M2—~20–24 Ma, M3—~18–9 Ma and M4—~9–6 Ma. Abbreviations defined in Figs. 1 and 2. Diagram has been constrained by >100 publications and the authors' interpretation within the Himalayan Metamorphic Front.

most workers have placed the Upper-Plate/Lower-Plate boundary at lower structural levels, coinciding with the Himalayan Unconformity in central and western Nepal (e.g. Hodges et al., 1996; Kohn et al., 2005; Fig. 4).

Throughout the central Himalaya, the Upper-Plate/Lower-Plate boundary occurs at structural levels higher than the Ramgarh Thrust (Pearson and DeCelles, 2005) or Main Central Thrust (MCT) as originally defined in India, Nepal and Bhutan (Heim and Gansser, 1939; Gansser, 1964, 1983). In central and western Nepal and into NW India, the Upper-Plate/Lower-Plate boundary at the base of the Tibetan Slab has also been named the MCT since the 1980s (e.g. Stöcklin, 1980; Hodges et al., 1988; Searle and Rex, 1989; Inger and Harris, 1992; Macfarlane et al., 1992; Hodges et al., 1996; Hubbard, 1996; Vannay and Hodges, 1996; Kohn et al., 2001, 2005; Pearson and DeCelles, 2005). Further west in NW India, the base of the Tibetan Slab is the Vaikrita Thust, at structural levels above the MCT or Ramgarh Thrust (Valdiya, 1980; Ahmad et al., 2000; Robinson et al., 2003). In eastern Nepal the base of the Tibetan Slab has been called the Kumbu Thrust or MCTII (Bordet, 1961; Hashimoto et al., 1973; Schelling, 1992; Lombardo et al., 1993; Pognante and Benna, 1993; Goscombe and Hand, 2000), the Chungthang Thrust or uppermost of two MCTs in Sikkim (Mohan et al., 1989; Catlos et al., 2004) and possibly also the Kakhtang Thrust, which is at higher structural levels than the MCT in Bhutan (Grujic et al., 1996; Davidson et al., 1997; Grujic et al., 2002; Daniel et al., 2003). To avoid confusion with the MCT at lower structural levels as originally defined, all

Fig. 6. Geological map of region investigated in eastern Nepal. Based on the authors mapping in 1992, 1997 and 2001 and Bordet (1961), Shrestha et al. (1984), Lombardo et al. (1993) and Pognante and Benna (1993). Structural symbols are main foliation and mineral aggregate stretching lineations. Abbreviations defined in Figs. 1 and 2 and J—Jonsong Peak. Note that in eastern Nepal the Himalayan Unconformity is sheared with strain equal to that pervasively distributed throughout the broad Main Central Thrust Zone (MCTZ). In the eastern Nepal study area the High Himal Thrust (HHT) marks the major, orogen architecture controlling structure between the Upper-Plate and Lower-Plate. Two new ε_{Nd} ratios determinations are indicated and typical of the Greater Himalayan Sequence (Parrish and Hodges, 1996). The range of ε_{Nd} ratios for the Lesser Himalayan Sequence is indicated in the stratigraphic column for comparison.

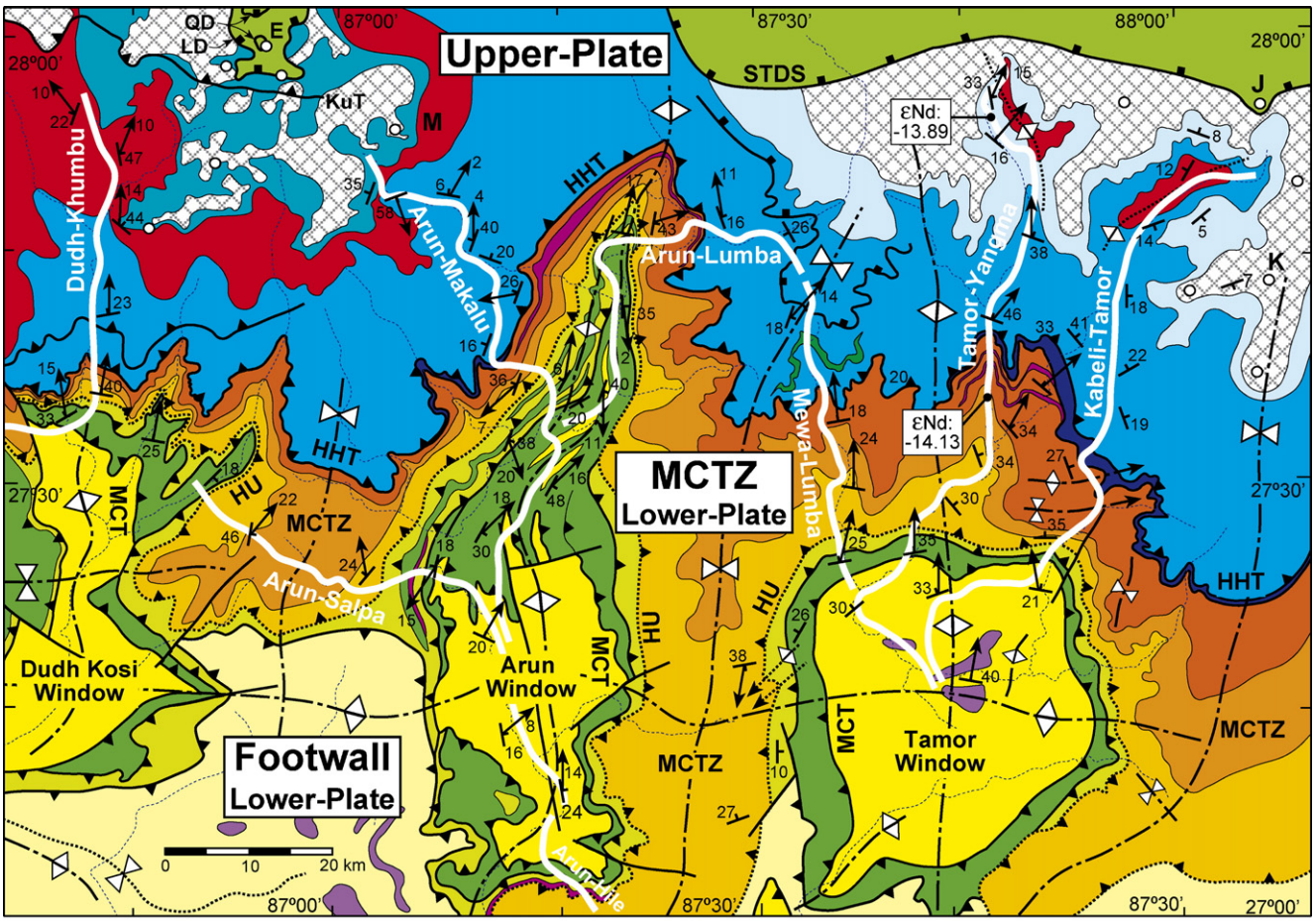
Upper-Plate
MCTZ
Lower-Plate
Footwall
Lower-Plate
STDS
HHT
MCT
HU
MCTZ
Dudh-Khumbu
Arun-Makalu
Arun-Lumba
Arun-Salpa
Mewa-Lumba
Tamor-Yangma
Kabeli-Tamor
εNd:
-13.89
εNd:
-14.13
Dudh Kosi
Window
Arun
Window
Tamor
Window
QD
LD
E
KuT
M
J
K
0 10 20 km
87°00'
87°30'
88°00'
28°00'
27°30'
27°00'

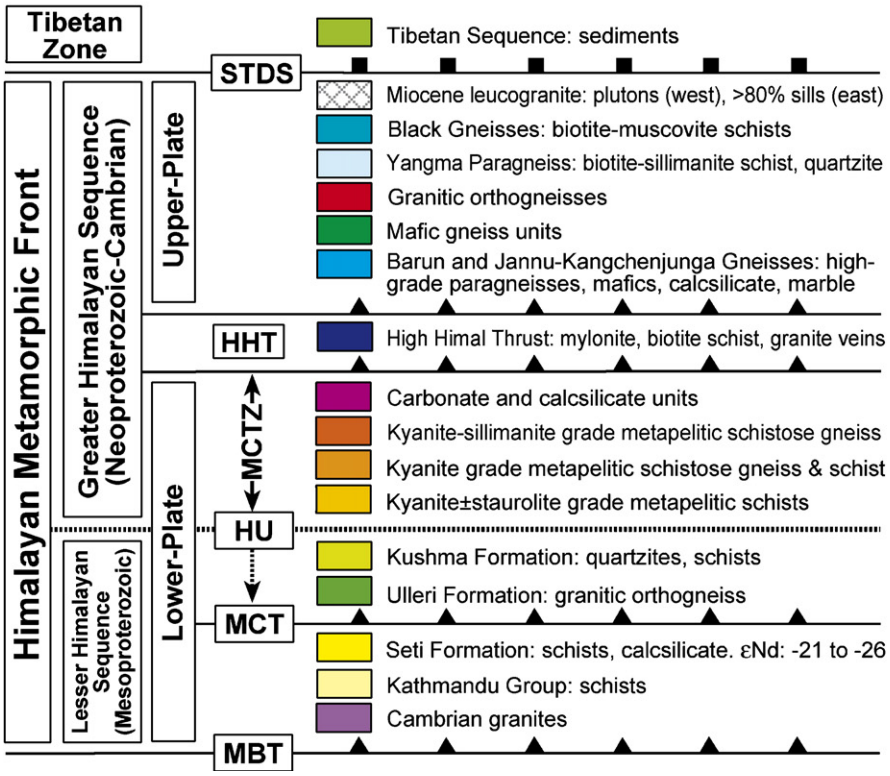
Tibetan Zone
Himalayan Metamorphic Front
Greater Himalayan Sequence (Neoproterozoic-Cambrian)
Lesser Himalayan Sequence (Mesoproterozoic)
Upper-Plate
Lower-Plate
STDS
HHT
MCTZ
HU
MCT
MBT
Tibetan Sequence: sediments
Miocene leucogranite: plutons (west), >80% sills (east)
Black Gneisses: biotite-muscovite schists
Yangma Paragneiss: biotite-sillimanite schist, quartzite
Granitic orthogneisses
Mafic gneiss units
Barun and Jannu-Kangchenjunga Gneisses: high-grade paragneisses, mafics, calcsilicate, marble
High Himal Thrust: mylonite, biotite schist, granite veins
Carbonate and calcsilicate units
Kyanite-sillimanite grade metapelitic schistose gneiss
Kyanite grade metapelitic schistose gneiss & schist
Kyanite±staurolite grade metapelitic schists
Kushma Formation: quartzites, schists
Ulleri Formation: granitic orthogneiss
Seti Formation: schists, calcsilicate. εNd: -21 to -26
Kathmandu Group: schists
Cambrian granites

sectors of the Upper-Plate/Lower-Plate boundary are collectively named the High Himal Thrust (HHT) (Figs. 1–4; Goscombe et al., 2003).

Southward extrusion of the Upper-Plate (Grujic et al., 1996; Vannay and Hodges, 1996; Davidson et al., 1997; Searle, 1999; Hodges et al., 2001, Stephenson et al., 2001; Beaumont et al., 2001; Grujic et al., 2002) was accommodated by coeval reverse movement on the HHT and top down to the north, normal reactivation of the STDS between ~22 and 10 Ma (Maluski et al., 1988; Hodges et al., 1996; Edwards and Harrison, 1997; Hodges et al., 1998; Harrison et al., 1999; Simpson et al., 2000; Godin et al., 2001). At structural levels below the HHT, the broad MCTZ and footwall was deformed at ~16–6 Ma (Macfarlane et al., 1992; Harrison et al., 1997; Huyghe et al., 2001; Robinson et al., 2001) and exhumed after ~11 Ma (Arita and Ganzawa, 1997; DeCelles et al., 1998). The Himalayan Metamorphic Front was thrust over late Miocene molasses of the Siwalik Group at the Main Boundary Thrust (LeFort, 1975; Robinson et al., 2001; Najman et al., 2005).

3. Methodology

Eight detailed profiles were mapped across the Himalayan Metamorphic Front in eastern Nepal (Figs. 6 and 7). These are; (1) along Dudh River into Kumbu region, (2) Arun River into Salpa Himal, (3) Arun and Barun Rivers into the Makalu region, (4) Arun and Medechheje Rivers into the Lumbasamba Himal, (5) Hile village into the Lower Arun valley, (6) Mewa River into Lumbasamba Himal, (7) Tamor and Yamga Rivers into Ohnmikangri Himal and (8) the Tamor and Kabeli Rivers in the Kangchenjunga region (Fig. 6). Semicontinuous profiles (Fig. 7) record stratigraphy, rock units, structural geometries, stretching lineations, kinematic indicators and qualitative and semi-quantitative estimates of bulk strain (Appendix A; Fig. 8). These profiles also record metamorphic mineral parageneses, leucosome and felsic intrusive types and their proportion in the rock mass was estimated in the field (Appendix B; Fig. 7). All stratigraphic thicknesses presented are based on altitude and since the Himalayan Metamorphic Front has an average unfolded dip of ~20° (Fig. 9), these consistently underestimate true stratigraphic thickness by only ~6%. Over 250 thin sections were examined to map metamorphic isograds (Appendix B). Two metapelite samples; one from within the MCTZ and another in the newly defined Yangma Paragneiss, were analysed for their isotopic Nd composition (Appendix C), to evaluate their provenance affinity with the Greater Himalayan Sequence. The rock units, deformation and metamorphism of the structural panels and bounding shear zones comprising the Himalayan Metamorphic Front are described from top to bottom.

4. Lithostratigraphic units

4.1. Miocene leucogranites

Although not strictly a lithostratigraphic unit, leucogranites comprise a significant component of the Upper-Plate. Garnet–muscovite–tourmaline±biotite±sillimanite leucogranite sills, dykes and plutons are ubiquitous late-stage intrusions, emplaced into the middle and upper levels of the Upper-Plate. Leucogranite is interpreted to have formed by decompressional partial melting of the Greater Himalayan Sequence during late peak metamorphism (Harris and Massey, 1994; Harris et al., 2004). The proportion of leucogranite preserved in the rock mass increases steeply to higher stratigraphic levels. Leucogranite is essentially absent below the HHT and only 1–2% of the section immediately above the HHT, typically as thin (5–20 cm) dykes and sills (Fig. 7). Middle levels, above 4000 m altitude, contain 10–20% leucogranite. Above 5000 m, the proportion increases rapidly from 40% to 60% and dominates the top 1300–2000 m of all profiles above 6000–6500 m altitude (Fig. 7; Appendix B). Leucogranites crystallized at 22–20 Ma in eastern Nepal (Simpson et al., 2000) and range in age between ~24 and 17 Ma elsewhere in the central Himalaya (e.g. Hodges et al., 1996; Edwards and Harrison, 1997; Hodges et al., 1998; Coleman, 1998).

4.2. Greater Himalayan Sequence

The Greater Himalayan Sequence is a thick (6000–6600 m) protolith package of high-grade metamorphics with Neoproterozoic (~800 Ma) to Cambrian ages (Parrish and Hodges, 1996; Upreti, 1999; Hodges, 2000; DeCelle et al., 2000; Robinson et al., 2001). In the Langtang region the age spectra of detrital zircons is 1000–800 Ma (Parrish and Hodges, 1996) and provenance is thought to be either from eastern Africa (DeCelle et al., 2000), or East Antarctica (Upreti and Yoshida, 2005). In eastern Nepal the Greater Himalayan Sequence has been informally subdivided into distinct rock units at different structural levels (LeFort, 1975). Most of these rock units are structurally bound and the stratigraphic relationship between them is largely unknown. The Greater Himalayan Sequence including leucogranite makes up 80–88% of the Himalayan Metamorphic Front, between the unconformity with the underlying Lesser Himalayan Sequence at 1000–2000 m altitude and the STDS at 7000–8000 m altitude (Fig. 7).

4.2.1. Black Gneisses and Yangma Paragneiss

The Black Gneisses (Lombardo et al., 1993) constitute the highest structural level in the Greater Himalayan Sequence below the leucogranite plutons in the Everest–Makalu region

Fig. 7. Eight profiles across the Himalayan Metamorphic Front in the eastern Nepal study area; representing stratigraphy, rock units, major structures, diagnostic mineral parageneses and metamorphic grade. The profiles are constructed from detailed mapping along sections by the authors and presented with respect to altitude (see text). Profile locations shown by white lines in Fig. 6. Red lines highlight the Himalayan Unconformity between the Lesser- and Greater Himalayan Sequences, the major HHT at the Upper-Plate/Lower-Plate boundary and the STDS. Diagnostic mineral abbreviations are after Kretz (1983) and additional abbreviations are; PM—migmatitic segregations, ph—phengite/sericite and fib—fibrolite. Qualitative representation of metamorphic grade indicated by black line width. However, for the Makalu and Kumbu traverses this is quantified to some extent (Fig. 12e, f).

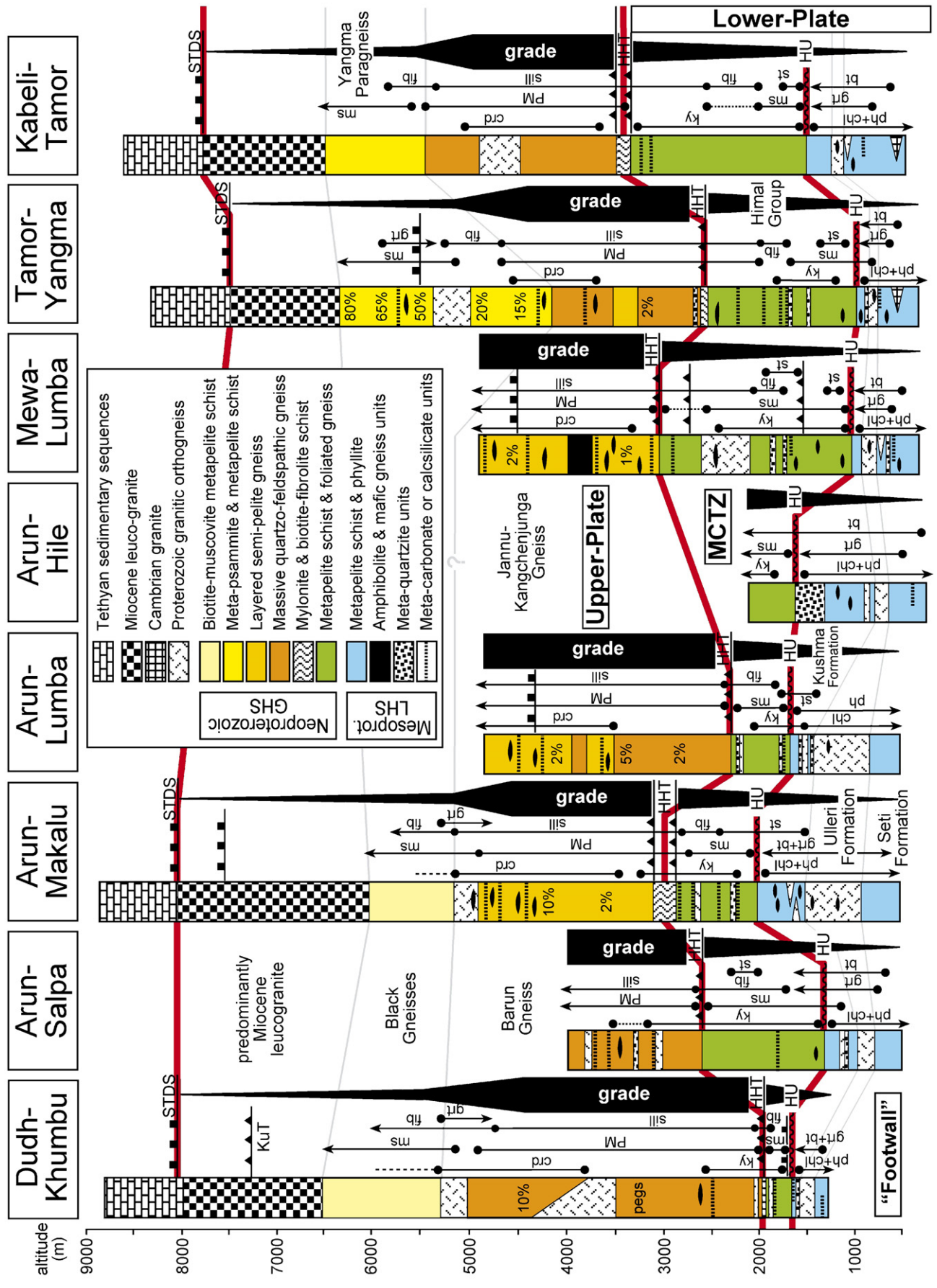
Kabeli-Tamor
Tamor-Yangma
Mewa-Lumba
Arun-Hile
Arun-Lumba
Arun-Makalu
Arun-Salpa
Dudh-Khumbu
altitude (m)
9000
8000
7000
6000
5000
4000
3000
2000
1000
Lower-Plate
Upper-Plate
"Footwall"
MCTZ
STDS
HHT
HU
grade
Yangma Paragneiss
Himal Group
Jannu-Kangchenjunga Gneiss
Kushma Formation
Ulleri Formation
Seti Formation
predominantly Miocene leucogranite
Black Gneisses
Barun Gneiss
KuT
pegs
Tethyan sedimentary sequences
Miocene leuco-granite
Cambrian granite
Proterozoic granitic orthogneiss
Neoproterozoic GHS
Mesoprot. LHS
Biotite-muscovite metapelite schist
Meta-psammite & metapelite schist
Layered semi-pelite gneiss
Massive quartzo-feldspathic gneiss
Mylonite & biotite-fibrolite schist
Metapelite schist & foliated gneiss
Metapelite schist & phyllite
Amphibolite & mafic gneiss units
Meta-quartzite units
Meta-carbonate or calcsilicate units

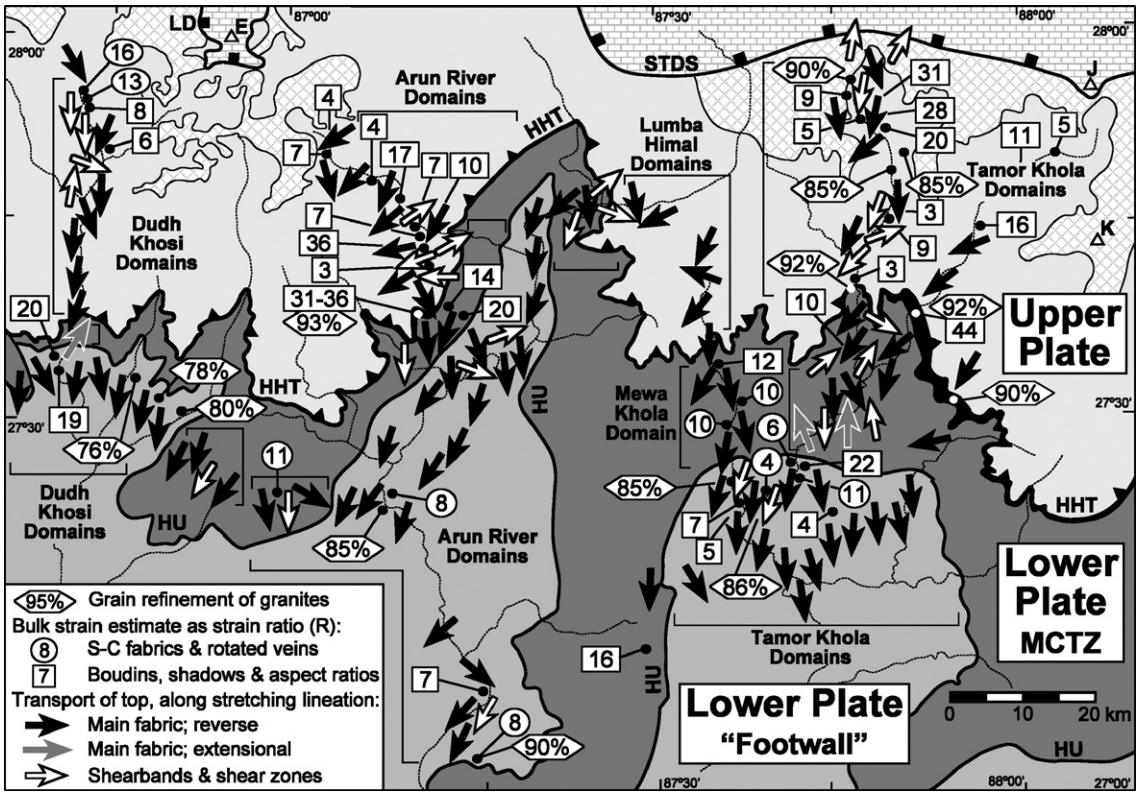

Fig. 8. Simplified geological map of eastern Nepal outlining structural domains referred to in Fig. 9. Arrows indicate transport of the top surface, along the trace of the local stretching lineation. Shear sense determined by asymmetric boudin trains, foliation oblique boudin trains, S–C fabrics, sigma-clasts, delta-clasts, C′-shear bands and flanking folds (Appendix A). Solid black and grey arrows are for the main foliation and hollow arrows are for later-stage shear bands and shear zones. Semi-quantitative estimates of bulk strain (Appendix A) are expressed as strain ratios (*R*). Strain ratios in rectangles are calculated from layer extension by boudinage, pressure shadows and aspect ratio of augens (Ramsay, 1967). Strain ratios in circles are converted from calculations of shear strain from angle of rotation of veins and angle between C- and S-planes (Ramsay and Graham, 1970). Degree of grain refinement of granite orthogneiss is presented in hexagons. All strain estimates are plotted in Fig. 13.

(Fig. 6). This metasedimentary sequence consists of biotite-rich schists containing muscovite, quartz, albite, K-feldspar, fibrolite and cordierite with minor foliated quartzo-feldspathic gneisses and quartzites (Brunel and Kienast, 1986; Lombardo et al., 1993; Pognante and Benna, 1993). The Yangma Paragneiss is an informally named 1000–2200 m thick unit of metasediments occurring at the highest structural levels in the Yangma and Tamor traverses, immediately below the zone of pervasive leucogranites (Fig. 6). Yangma Paragneiss is a monotonous sequence of amphibolite facies metaquartzite, metapsammite and metapelite schists (Fig. 10b) with rare amphibolite, and is devoid of calcsilicate. This unit is at the same structural level as the Black Gneisses and share gross lithological similarities and metamorphic mineral parageneses.

4.2.2. Barun Gneiss and Jannu-Kangchenjunga Gneiss

Barun Gneiss is defined in the Everest–Makalu region (Bordet, 1961; Brunel and Kienast, 1986; Lombardo et al., 1993; Pognante and Benna, 1993), and consists of upper-amphibolite to granulite facies quartzo-feldspathic, metapelitic, mafic and calcsilicate rocks. Coarse-grained, layered and migmatized garnet–biotite±sillimanite quartzo-feldspathic units dominate with minor garnet–cordierite–sillimanite metapelite (Fig. 10b). Bands of garnet–hornblende±clinopyroxene mafic gneiss and carbonate and calcsilicate containing clinopyroxene, wollastonite, forsterite and scapolite occur throughout the unit. The Jannu-Kangchenjunga Gneiss is described from the Kangchenjunga region in the far east of Nepal and Sikkim (Mohan et al., 1989). Also dominated by garnet–sillimanite±cordierite migmatites with minor mafic, carbonate, calcsilicate and quartzite, this unit is similar to and laterally equivalent to the Barun Gneiss (Fig. 6; Goscombe and Hand, 2000). These two rock units comprise the high-grade portion of the Greater Himalayan Sequence, and make up 30–50% of its structural thickness above the HHT, the remainder being lower-grade units and leucogranite at high structural levels (Fig. 7). Identical, high-grade migmatitic gneisses at the same structural level continue eastward as Darjeeling Gneiss in Sikkim (Dasgupta et al., 2004; Harris et al., 2004) and into Bhutan (Swapp and Hollister, 1991; Grujic et al., 2002; Daniel et al., 2003).

4.2.3. Granitic orthogneisses

Granitic orthogneiss sheets occur at multiple structural levels within the Barun–Jannu-Kangchenjunga Gneiss and Yangma Paragneiss units (Figs. 6 and 7). The Namche Migmatite Orthogneiss (Lombardo et al., 1993) in the Everest–Makalu region is sheared biotite–granite augen orthogneiss with

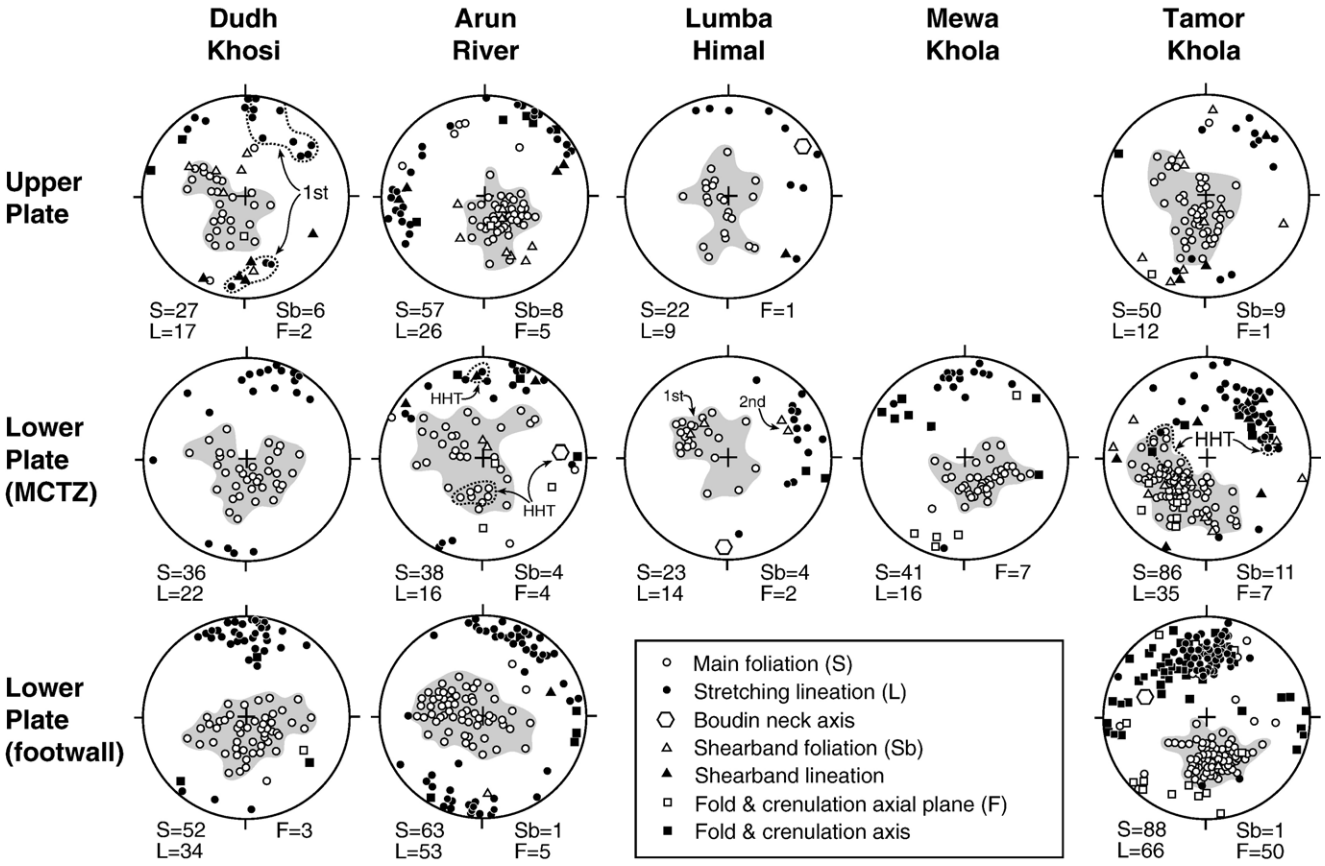

Fig. 9. Lower hemisphere equal-area projections of structural data from the domains outlined in Fig. 8. The shaded region outlines poles to the main foliation. Structural data from the High Himal Thrust (HHT) is outlined by dashed line.

interlayered migmatized biotite–sillimanite quartzo-feldspathic gneiss and minor calcsilicate, carbonate and garnet mafic gneiss (Pognante and Benna, 1993). Further east is an ~400 m thick unit of biotite±garnet granite orthogneiss within the Yangma Paragneiss in the Yangma River, and at lower structural levels biotite–sillimanite granite augen orthogneiss within Jannu-Kangchenjunga Gneiss in the Tamor River (Figs. 6 and 7). U–Pb zircon, monazite and xenotime ages suggest emplacement at 465–470 Ma in the Everest–Makalu region (Viskupic and Hodges, 2001) and 484±9 Ma in the Annapurna region (Godin et al., 2001).

4.2.4. Greater Himalayan Sequence within the Main Central Thrust Zone

Below the HHT and above the Himalayan Unconformity bounding the Lesser Himalayan Sequence is a 350–1900 m thick sheared and thrusted package of amphibolite facies metapelite and semi-pelite schist and gneiss with minor calcsilicate, quartzite and amphibolite (Figs. 6 and 7). This package constitutes the inverted metamorphic sequence of the MCTZ between the HHT and Himalayan Unconformity. In eastern Nepal rocks within the MCTZ are basal units of the Greater Himalayan Sequence called the Himal Group and at lower structural levels, the Kathmandu Group (Bordet, 1961; Shrestha et al., 1984; Lombardo et al., 1993). The Greater Himalayan Sequence in the MCTZ thickens eastward, from ~350 m in the Everest region to ~1900 m across eastern Nepal (Fig. 7) into Sikkim–Bhutan (Figs. 1 and 2).

In all traverses the Himalayan Unconformity has been mapped lithostratigraphically (Colchen et al., 1986). The unconformity is marked by an abrupt transition in rock types; from pale, fine-grained, Na- and Ca-poor quartz–sericite schists with graphitic phyllonites of the Lesser Himalayan Sequence, immediately above the Ulleri Formation orthogneiss, up into Himal Group with its more typical metapelite, meta-greywacke and thick carbonate units (Fig. 7). The Himal Group varies from garnet–biotite–muscovite–albite–quartz schists at lowest levels up to garnet–biotite–bytownite–K-feldspar–kyanite foliated gneiss. Matrix sillimanite and rare leucosome segregations with paratactic garnet only occur at highest levels (Lombardo et al., 1993; Goscombe and Hand, 2000). Quartzite units up to 20 m thick and thin (10–200 cm) units of epidote– to clinopyroxene–amphibolite, calcsilicate and carbonate are widely distributed. Thick (≤100 m) units of banded clinopyroxene–garnet calcsilicate represent local variation in the Himal Group (Figs. 6 and 7).

Nd-isotope analysis of two metapelite samples from the Tamor–Yangma traverse were undertaken to confirm the extent of the Greater Himalayan Sequence, both below the HHT within the MCTZ and at the highest stratigraphic level (Fig. 6). $\varepsilon_{Nd}(0)$ from Yangma Paragneiss is −13.9 above the HHT and −14.1 from Himal Group below the HHT (Fig. 6; Appendix C). These

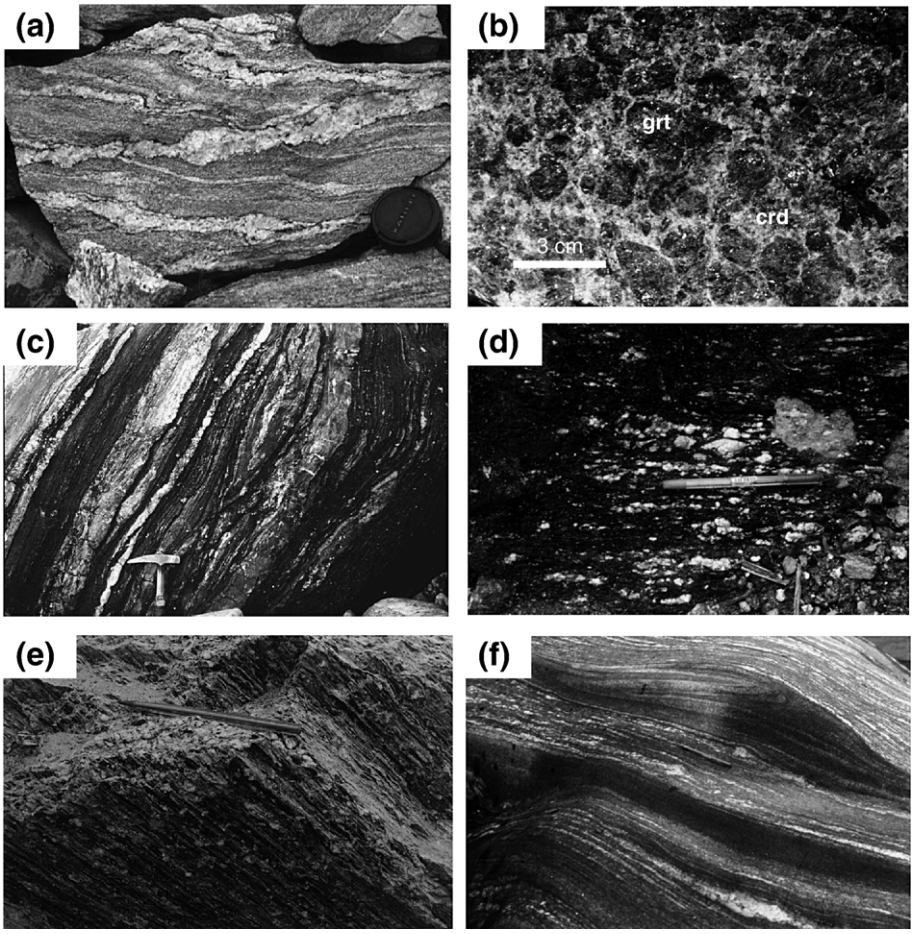

Fig. 10. Deformation fabrics across the Himalayan Metamorphic Front: locations in Fig. 12d. (a) Migmatized high-grade cordierite semi-pelite gneiss with two generations of leucosomes in the Upper-Plate (location J27). Boulder is out of situ. (b) Coarse-grained polygonal granoblastic garnet–cordierite granulite from the Upper-Plate (location M31). Looking to the north. (c) Attenuated compositional layering and intense foliation development in Yangma Paragneiss in the Upper-Plate (location T97). Looking east at a steep outcrop. (d) Strong foliation intensity, high degree of grain-refinement and pervasive disaggregation of granitic segregations in mylonitized biotite–quartzofeldspathic gneiss within the HHT (location M130). Looking to the northwest on a horizontal platform. (e) Intense grain-refinement of Ulleri Formation granitic orthogneiss, now biotite–muscovite foliated augen gneiss, within the Lower-Plate (location KN64). Looking to the west. (f) Intense transposed foliation and intrafolial folds in metapelite schists within MCTZ of the Lower-Plate (location T31). Looking to the north on a horizontal platform.

$\varepsilon_{Nd}(0)$ values are typical of the Greater Himalayan Sequence from elsewhere in the central Himalaya, and do not overlap with the Lesser Himalayan Sequence (Parrish and Hodges, 1996; Ahmad et al., 2000; Robinson et al., 2001; Martin et al., 2005 and references cited therein). The structurally lower sample confirms that metasediments in the MCTZ are part of the Greater Himalayan Sequence, and that the HHT is located within the Greater Himalayan Sequence and does not coincide with an unconformity.

4.3. Lesser Himalayan Sequence

The Lesser Himalayan Sequence is exposed only at lowest structural levels in the Himalayan Metamorphic Front, within antiformal tectonic windows incised by the Dudh, Tamor and Arun Rivers (Fig. 6). The Lesser Himalayan Sequence is represented in central Nepal by the Kuncha Formation (Stöcklin, 1980), and in eastern Nepal by the Midland Group, which consists of metasedimentary Kushma and Seti Formations and Ulleri Formation orthogneiss (Shrestha et al., 1984). Elsewhere in the central Himalaya, the Lesser Himalayan Sequence has been interpreted as a Palaeo- to Mesoproterozoic basinal sequence, possibly as old as ~1870–1600 Ma, deposited on the Indian Plate (Parrish and Hodges, 1996; Upreti, 1999; Hodges, 2000; DeCelle et al., 2000; Miller et al., 2000; Robinson et al., 2001). In the Langtang region the peaks of detrital zircon ages range between 2600 and 1870 Ma (Parrish and Hodges, 1996) with a suggested Indian Craton provenance (DeCelle et al., 2000; Upreti and Yoshida, 2005). The Lesser Himalayan Sequence has ε_{Nd} values between −26 and −20, and is distinct from the less evolved overlying Greater Himalayan Sequence (Parrish and Hodges, 1996; Ahmad et al., 2000; Robinson et al., 2001; Martin et al., 2005 and references cited therein).

4.3.1. Kushma Formation

The Kushma Formation (Shrestha et al., 1984) is a thin (100–750 m) package of metasedimentary rocks at the top of the Lesser Himalayan Sequence immediately above Ulleri Formation orthogneiss. The package consists of quartz–sericite schist and metaquartzite with subordinate amphibolite schist,

actinolite calcsilicate and graphitic phyllonite. Meta-quartzite units are typically <10 m and packages are up to 200 m thick. The quartz–sericite schists are medium-grained, pale grey and of similar appearance to the Seti Formation at lower structural levels. Both have garnet but the Kushma Formation differs slightly by being less phyllonitic and more schistose with a higher proportion of albite, biotite and rarely also kyanite.

4.3.2. Ulleri Formation

The Ulleri Formation is a 200–600 m thick laterally continuous granitic orthogneiss sheet that is in part structurally repeated (Figs. 6 and 7). This granitic orthogneiss typically has protomylonitic to mylonitic fabrics with perthitic K-feldspar augen enveloped by a foliated matrix of muscovite–biotite–quartz–plagioclase–K-feldspar (Fig. 10e). Sub-parallel amphibolite schists of 1 m width are interpreted as transposed mafic dykes. The basal Ulleri Formation is a strongly interleaved package of sheared orthogneiss and muscovite–biotite±garnet metapelite schists of the Seti Formation. Ulleri Formation is a semicontinuous unit found through all of Nepal, and interpreted to be approximately 1850 Ma in age (Robinson et al., 2001).

4.3.3. Seti Formation

The Seti Formation (Shrestha et al., 1984) is a monotonous sequence of fine-grained, pale grey-green sericite–quartz± albite±chlorite schists and phyllonite. At highest structural levels immediately below the Ulleri Formation, these schists contain post-kinematic biotite laths and syn-kinematic garnets (Meier and Hiltner, 1993). Rare thin (10–100 cm) layers of amphibolite schist, plagioclase–epidote–actinolite calcsilicate, micaceous marble and quartzite are widespread.

5. Structural architecture

5.1. South Tibet Detachment System

The South Tibet Detachment System (STDS; Figs. 1 and 2) is a shallow, north-dipping zone of low-grade ductile shear zones and brittle faults with top down to the north, normal movements, between Greater Himalayan Sequence and Tethyan Sequence (Burg et al., 1984; Burchfiel et al., 1992; Searle, 1999; Law et al., 2004). In eastern Nepal the STDS occurs at altitudes between 7000 and 8000 m and is consequently not mapped in this study. Discrete normal-fault detachments and km-scale foliation boudinage are recognised in cliffs at altitudes >6500 m in the Yangma, Makalu and Jonsong Himals, at the highest structural levels in the Upper-Plate (Fig. 6). The STDS outcrops almost entirely in Tibet, and within eastern Nepal only in the summits of Mount Everest (Searle, 1999; Law et al., 2004) and Jonsong Peak north of Kangchenjunga (Smythe, 1930). At Mount Everest the STDS is comprised of two discrete detachments (Fig. 6), the Lhotse Detachment and at higher structural levels, the younger Qomolangma detachment (Searle, 1999; Searle et al., 2003). The same geometry is observed in Bhutan (Grujic et al., 1996) and in the Annapurna–Manaslu region (Searle and Godin, 2003). At Jonsong Peak the STDS is a zone of shear-interleaved gneisses of the Greater Himalayan Sequence and Tethyan Sequence limestone (Smythe, 1930). Elsewhere, leucogranite intrudes across the STDS and is deformed, indicating normal-fault reactivation of the STDS from ~22–17 Ma (e.g. Murphy and Harrison, 1999; Searle, 1999; Harrison et al., 1999; Godin et al., 1999, 2001) to ~11 Ma (Maluski et al., 1988; Edwards and Harrison, 1997; Wu et al., 1998).

5.2. Upper-Plate deformation

The Upper-Plate (Fig. 3) is composed of medium- to high-grade migmatites of the Greater Himalayan Sequence, with typically coarse-grained, differentiated gneissic fabrics (Fig. 6). These rocks preserve several generations of migmatization (Fig. 10a; Appendix B), deformation fabrics, lineations and folds, and have been overprinted by mid-amphibolite facies shear bands and shear zones (Fig. 11). Prograde fabrics are preserved as crenulated sillimanite inclusion trails in garnet porphyroblasts. An apparently protracted deformation and metamorphic history, and the complex structures contrast with the simple geometries in the Lower-Plate.

Gross compositional layering, gneissic layering and both concordant and discordant garnet-bearing migmatitic segregations are attenuated (Fig. 10a) and boudinaged during development of a pervasive penetrative foliation. The main foliation defined by biotite, sillimanite and aggregate ribbons is typically parallel to lithologic layering and dips shallowly (20–40°) N, NE and NW (Fig. 9). Migmatitic segregations associated with main phase deformation accumulated in inter-boudin necks and pressure shadows around porphyroclasts. Leucogranite veins and late-stage biotite–pegmatite veins cross cut the main foliation (Fig. 11). A bimodal distribution of poorly developed mineral and mineral aggregate lineations within the main foliation plunge N–NE and NW–W (Fig. 9). Stretching lineation orientations and shear sense indicators such as S–C composite fabrics, asymmetric boudins and mantled porphyroclasts indicate a complex kinematic array of top to the S and SW reverse transport (Fig. 8). Top down to the north, normal transport associated with the main fabric has not been recognised (Fig. 8).

The main foliation is folded by multiple fold generations, the dominant being tight to isoclinal folds without significant axial planar foliation development and with shallow plunges to the NNE and NW to W (Fig. 9). Sillimanite, biotite and gedrite-bearing shear zones (cm-scale) and shear bands (mm-scale) overprint the main fabric at low angles. These are dominated by reverse, top to the S and SW transport (Fig. 8). Shear zones and shear bands with normal-fault movements of top down to the N, NE or E occur in two settings; within or immediately above the HHT, and at the highest structural levels visited in this study, approximately 2500 m below the STDS (Fig. 8). All the above fabrics are folded by late-stage tight to close folds and associated crenulations that plunge shallowly NNE to NE.

5.3. High Himal Thrust

The 100–400 m thick HHT is an intensely sheared zone that marks both a fundamental discontinuity in deformation style and is the median structure in a zone of rapid change in metamorphic

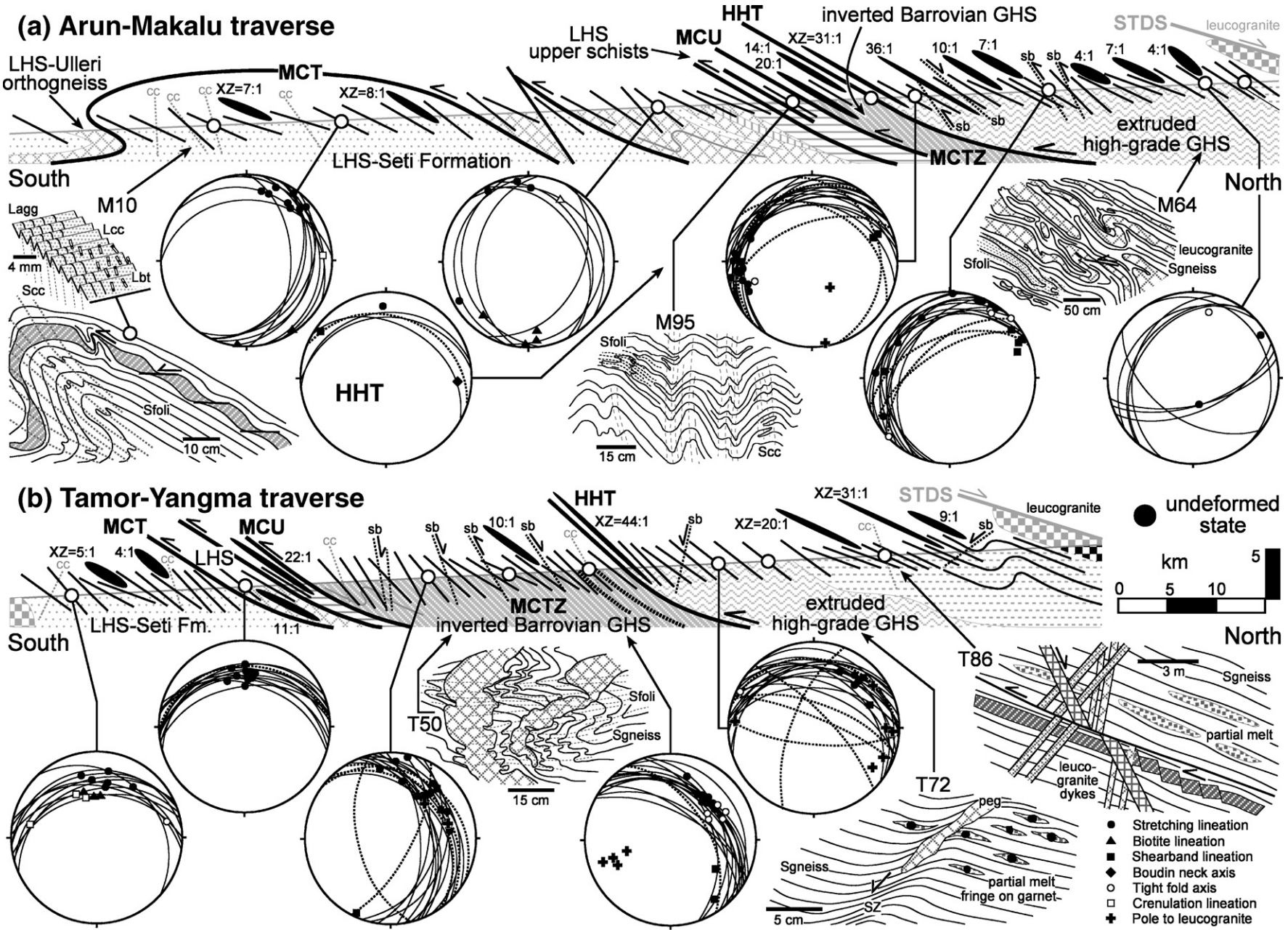

Fig. 11. Representative structural profiles across the Himalayan Metamorphic Front in eastern Nepal: (a) Arun-Hile to Arun-Makalu profile and (b) Tamor–Yangma profile (Fig. 6). Lower-hemisphere, equal area stereonets of structural data and outcrop observations are from select localities. Thin great circles are main foliation and thick, dashed great circles are shear bands and shear zones. Bulk strain data expressed as the *X*/*Z* strain ratio (*R*) and shown by the shape and orientation of the black strain ellipse. Abbreviations used: Scc—crenulation cleavage, Lcc—crenulation lineation, Sfoli—main foliation, Lbt—biotite lineation, Lagg—mineral aggregate stretching lineation, Sb—shear band and Sgneiss—gneissic fabric.

grade. This structure represents the Upper-Plate/Lower-Plate boundary within the Himalayan Metamorphic Front in eastern Nepal (Goscombe et al., 2003). This structure is similar in character and laterally continuous across eastern Nepal (Figs. 6 and 8). The HHT contains 10–20% relict migmatitic segregations (Fig. 10d), indicating reworking and downgrading of the high-grade migmatitic Greater Himalayan Sequence. The mylonitic foliation envelops garnet and feldspar porphyroclasts with sillimanite inclusions preserving early fabrics. Porphyroclasts were grain-refined by dynamic recrystallization and resorption by metamorphic reactions. Intense grain refinement of >90% of the rock and grain size reduction by recrystallization produced medium- to fine-grained biotite-rich schists and mylonites with aligned biotite, sillimanite and quartz–feldspar aggregate ribbons. Pre-existing migmatitic segregations and granite veins are grain-refined and stretched into disaggregated lenticular lenses (Fig. 10d). The HHT dips 20–40° to the N, ENE and NW and stretching lineations plunge down-dip to the N and ENE (Figs. 6, 8 and 9). Asymmetric boudinage and C′-shear bands indicate N over S shear sense in the HHT. The mylonitic fabric is isoclinally folded and overprinted by thin, late-stage biotite-seams and shear bands with both reverse and normal shear sense. The HHT is easily eroded, poorly exposed and marks a break in slope to steeper terrane in the overlying resistant Barun–Jannu-Kangchenjunga Gneisses.

5.4. Lower-Plate deformation

Greater Himalayan Sequence rocks above the Himalayan Unconformity and within the MCTZ (Fig. 3) are characterized by homoclinal NE- to NW-dips (20–30°) and transposed parallel layering and schistosity (Figs. 6, 8 and 10c, f). This zone represents a broad domain of shear during the development of peak metamorphic mineral parageneses containing biotite, muscovite, kyanite and aggregate ribbons that define the main foliation. Progressive shortening across the foliation resulted in enveloped porphyroclasts, pressure shadows and strained and boudinaged peak metamorphic minerals. Across the MCTZ, fabrics change smoothly from fine- to coarse-grained schist to schistose gneiss and gneiss at the top. The main foliation is parallel to thrusts, gross compositional layering and also the metamorphic isograds, as far as can be determined by mapping. Lesser Himalayan Sequence rocks in the footwall tectonic windows below the Himalayan Unconformity have phyllonitic to fine-grained schist foliations. Thrust repetition of rock units such as quartzite and Ulleri Formation is recognised in the Salpa Himal and Arun River traverses (Figs. 6 and 7; Bordet, 1961; Lombardo et al., 1993) and there is repetition of metamorphic zonation in the Mewa River traverse (Fig. 7). Mylonites with higher than background strain (Fig. 10e, f) are recognised within and immediately above and below the Ulleri Formation in all traverses, and correlate with the structural level of the MCT (Shrestha et al., 1984).

Aligned kyanite, biotite, muscovite and hornblende and mineral aggregate stretching lineations are well developed in most rock types. Stretching lineations show mono-modal orientation parallel to dip and kinematic indicators such as S–C and S–C′ composite foliations, asymmetric boudins and sigma-clasts consistently indicate north over south, reverse movement (Fig. 8). Of 235 shear sense determinations in the vicinity of the MCT, all except 3 are reverse (Appendix A). Strike orthogonal reverse transport is characteristic of the MCTZ throughout the central Himalaya (Shackleton and Ries, 1984; Vannay and Hodges, 1996; Grujic, et al., 2002). Top down to the north, normal movements are indicated by C′-shear bands associated with the main fabric in only three localities, all immediately above the Himalayan Unconformity (Fig. 8). Later formed, shear bands are discrete mm-scale fine-grained biotite seams with quartz-aggregate ribbons and also fibrolite at the highest structural levels immediately below the HHT. High in the MCTZ, late-stage shear bands dip 30–50° to the NE and SW and dip 60–70° to the N at lower structural levels (Figs. 9 and 11). These late-stage shear bands have both reverse and normal shear sense; earliest formed show top to the S and SW, and the latest show top down to the NE or E (Fig. 8).

The main foliation is folded and crenulated by shallowly inclined, asymmetric tight to isoclinal folds with S-vergence and sub-horizontal E–W to ESE–WNW trending hinges orthogonal to stretching lineations (Fig. 9). South verging and N to NE dipping (60–80°), tight to close folds have retrograde axial planar crenulation cleavages containing muscovite–biotite±chlorite (Figs. 9 and 11). Latest formed, close to open, upright mesoscopic folds and crenulations plunge shallowly to the NNE, NE and SW and have aligned biotite laths (Fig. 9). This latest episode of folding is interpreted to be associated with large-scale warping of Upper- and Lower-Plates, resulting in erosional windows that expose footwall rocks in the major antiforms sited at the Dudh, Arun and Tamor Valleys (Fig. 6).

5.5. Strain gradient

Semi-quantitative estimates of bulk strain utilizing aspect ratios of conglomerate clasts and stretched augen (Ramsay, 1967), boudin train extension (Goscombe et al., 2004), the angle between composite S–C foliations (Ramsay and Graham, 1970) and pressure fringes such as quartz fibres or partial melt where there has been extension of the matrix adjacent to porphyroclasts (Hobbs et al., 1983) are all presented in Figs. 8 and 11 and Appendix A. All methods assume plane strain and for comparison across the region, shear strain estimates have been normalized to strain ratio (R) assuming simple shear (Fig. 8). All values are considered minimum estimates of strain due to internal deformation of clasts and boudins, competency contrast between clast and matrix, influence of pre-deformation clast shape and all markers recorded only a portion of the strain history. In particular stretched augen significantly underestimate bulk strain due to recrystallization and mortor development (Schmid and Podladchikov, 2004). A more continuous profile of qualitative strain based on foliation intensity, indicated by aspect ratio and spacing of planar elements and degree of grain refinement, was documented for each traverse (Appendix A). This qualitative representation also underestimates bulk strain, mainly because only the last component of a progressive strain history is preserved and at higher metamorphic grades, foliations are inherently less well

developed due to feldspar growth in preference to micas as well as annealing processes. Nevertheless, together these qualitative profiles and semi-quantitative estimates give a semicontinuous picture of bulk strain variation across the Himalayan Metamorphic Front in eastern Nepal.

Moderately high strain ratios of 4–20 are distributed across the Lower-Plate and both strain ratio estimates and foliation intensity increase on average up through the MCTZ towards the HHT (Figs. 8 and 11). A similar strain gradient is recognised in Bhutan (Grujic et al., 1996, 2002). Repetition of stratigraphic units and metamorphic zonation in some traverses (Fig. 7) indicate the presence of thrusts and some degree of strain heterogeneity in the MCTZ. High strain ratios of 16–20 are recorded below the Himalayan Unconformity, both within (Fig. 10e) and immediately adjacent to (Fig. 10f) the Ulleri Formation (Figs. 8 and 11). These represent a zone of higher than background strain that correlates with the MCTI (Hashimoto et al., 1973; Arita, 1983), at the same structural level as the originally defined MCT (Heim and Gansser, 1939; Gansser, 1964, 1983). At higher structural levels, there is no marked strain gradient in the vicinity of the Himalayan Unconformity, across which strain is equally partitioned, and foliation intensity does not change. Similarly there is no change in structural style or orientation of the main foliation or stretching lineation across the unconformity (Fig. 9). Consequently, there is no evidence for a major crustal structure coincident with the Himalayan Unconformity in eastern Nepal.

In contrast, markers in the Upper-Plate record typically lower strain ratios of 3–10 due to annealing, and a very heterogeneous strain distribution with strain ratios up to 20–36 in discrete m-scale shear zones (Figs. 8 and 11). At highest structural levels beyond observations made in this study, moderate strain ratios ($R \leq 6.0$) and high pure shear component of flow ($Wk \approx 0.7$) are recorded immediately below the STDS (Law et al., 2004). Superimposed on top of the first-order, regional strain distribution, very high strains are partitioned into the HHT where strain ratios of 30–45 are recorded by pressure fringes on garnet porphyroblasts and extreme boudinage of granite veins and calcsilicate layers (Figs. 8 and 11; Appendix A). Grain refinement of >90% of the rock, intense disaggregation of layering and pervasive ductile mylonite fabrics across the whole width of the HHT define the only large-scale (100–400 m wide) and strongly partitioned high strain zone in the Himalayan Metamorphic Front.

6. Metamorphic architecture

6.1. Upper-plate metamorphism

Barun and Jannu-Kangchenjunga Gneisses have granulite facies (Figs. 10a and 12d) metapelites with peak metamorphic assemblages of garnet–sillimanite±cordierite–K-feldsparbiotite–quartz–plagioclase±rutile (Brunel and Kienast, 1986; Lombardo et al., 1993; Pognante and Benna, 1993; Goscombe and Hand, 2000). Highest-grade rocks formed at 837±59 °C and 6.7±1.0 kbar, defining a T/depth ratio of ~36 °C/km (Goscombe and Hand, 2000). Granulite facies conditions of 800–850 °C and 10–12 kbar continue east into Sikkim (Neogi et al., 1998; Dasgupta et al., 2004; Harris et al., 2004) and Bhutan (Swapp and Hollister, 1991; Davidson et al., 1997). Peak metamorphic garnets are compositionally flat and typical of homogenisation at high grades (Goscombe and Hand, 2000; Dasgupta et al., 2004). The Prograde P–T evolution has not been confidently established. Sillimanite–hercynite inclusion assemblages implying early low pressure conditions (Goscombe and Hand, 2000) are incompatible with both the high pressures reported from similar structural levels in Sikkim (e.g. Harris et al., 2004) and cordierite moats on garnet indicating decompression through the peak-T of metamorphism (Davidson et al., 1997; Goscombe and Hand, 2000). Sillimanite–gedrite–biotite assemblages occur in late-stage shear bands and replace cordierite, suggesting isobaric to shallow $-\Delta P$ cooling paths (Fig. 12b, c; Goscombe and Hand, 2000).

Matrix assemblages indicate a systematic variation in metamorphic grade across the Upper-Plate. Basal Upper-Plate in the Everest–Makalu region contains garnet–sillimanitekyanite± rutile metapelite migmatites (Lombardo et al., 1993; Pognante and Benna, 1993). East of the Arun River, kyanite parageneses are absent in the Upper-Plate and there is a sharper metamorphic transition with the underlying Lower-Plate (Fig. 7). In all profiles, the highest-grade cordierite–granulite assemblages are restricted to 3500–5000 m altitude in the lower half of the Upper-Plate (Figs. 7 and 12d, e, f). Above 5000 m there is a rapid decrease in metamorphic temperature and pressure in the Black Gneisses and Yangma Paragneiss units (Fig. 12d). This is marked by incoming fibrolite and muscovite, absence of migmatization and coarse sillimanite and the transition at higher levels (~6000 m) to decreasing garnet, increasing muscovite and absence of K-feldspar, fibrolite, garnet and cordierite (Fig. 7; Brunel and Kienast, 1986; Hubbard, 1989; Lombardo et al., 1993; Pognante and Benna, 1993; Goscombe and Hand, 2000). Cordierite–biotite–muscovite–K-feldspar–fibrolite schists indicate peak-T conditions of ~650–700 °C and ~4–6 kbar (Hubbard, 1989; Lombardo et al., 1993; Goscombe and Hand, 2000). A similar rapid decrease in T and P at the highest structural levels in the Upper-Plate has been reported from central Nepal (Pêcher, 1989; Macfarlane, 1995; Fraser et al., 2000).

U–Pb age determinations from peak metamorphic parageneses in the Everest region indicate matrix monazite and xenotime growth at 22–23 Ma (Simpson et al., 2000) and ~25 Ma (Viskupic and Hodges, 2001). Leucogranites generated during peak metamorphic melting have monazite and xenotime ages of 20–22 Ma (Simpson et al., 2000) and elsewhere; 25–21 Ma in central Nepal (e.g. Coleman, 1998) and 23–22 Ma in Sikkim (Harris et al., 2004; Catlos et al., 2004) and Bhutan (Daniel et al., 2003). Eohimalayan metamorphism, recorded by monazite inclusions in garnet, has ages of 31–32 Ma in the Everest region (Simpson et al., 2000) and 32–35 Ma in the Annapurna region (Godin et al., 2001).

6.2. High Himal Thrust metamorphism

Mylonites within the HHT show a complex metamorphic evolution; early high-grade parageneses are evident as relict

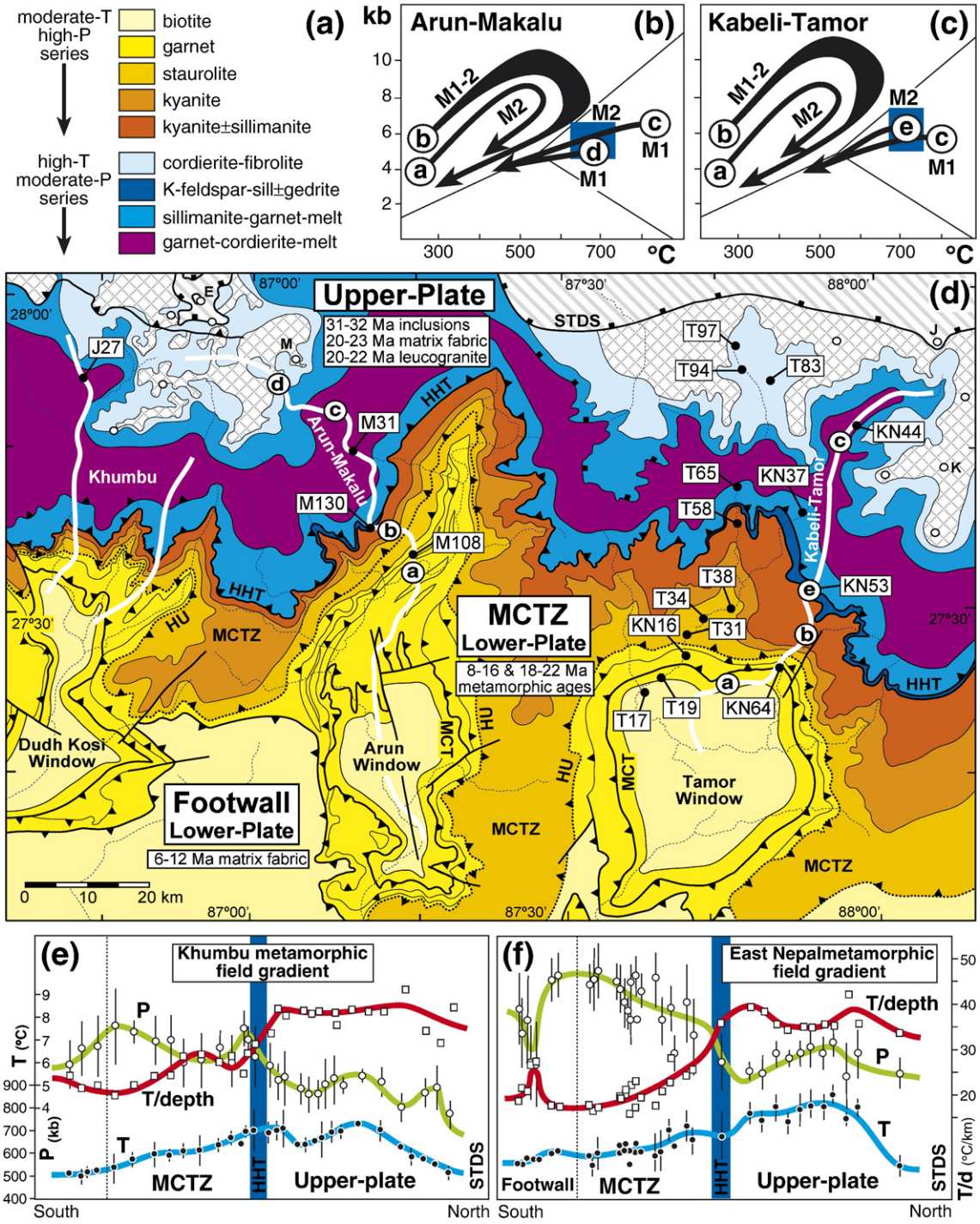

Fig. 12. Metamorphic architecture of eastern Nepal. (a) Legend of diagnostic mineral fields represented in (d). (b, c) *P–T* paths from different parts of the Himalayan Metamorphic Front as indicated in (d) (Goscombe and Hand, 2000). (d) Simplified metamorphic map of peak metamorphic matrix assemblages (Appendix B). Blues and purples represent high-*T*/moderate-*P* metamorphic series and yellows and oranges represent moderate-*T*/high-*P* series. Age constraints in the different structural-metamorphic domains are based on U–Th–Pb ages from monazite, xenotime and uraninite from the Everest region (Simpson et al., 2000) and localities approximately 160 and 200 km to the west in central Nepal (Harrison et al., 1997; Kohn et al., 2001). Sample localities referred to in Fig. 10 are indicated in boxes. Small circles are mountain peaks. (e, f) Composite metamorphic field gradients based on published *P–T* data (Appendix B). (e) Khumbu metamorphic field gradient (Hubbard and Harrison, 1989; Hubbard, 1989; Pognante and Benna, 1993). (f) East Nepal metamorphic field gradient (Pognante and Benna, 1993; Goscombe and Hand, 2000). Peak metamorphic conditions are not necessarily time equivalent along field gradients, as indicated by the age constraints in (d). The *T* (°C)/depth (km) ratio was calculated assuming an average rock density of 2.8 g/cm^3.

porphyroclasts of K-feldspar and garnet with sillimanite inclusions, and enveloped lenses of felsic segregation. Intense reworking and grain refinement by pervasive recrystallization and grain size reduction produced a penetrative foliation with sillimanite–biotite–quartz–plagioclase±garnet±gedrite assemblages that formed at 674±33 °C and 5.7±1.1 kbar (Fig. 12b, c; Goscombe and Hand,

2000). Identical assemblages are developed in shear bands and shear zones that cross cut the main fabric in the uppermost MCTZ and throughout the high-grade portion of the Upper-Plate.

6.3. Lower-Plate metamorphism

6.3.1. Main Central Thrust Zone

All profiles show near smooth and continuous increase in metamorphic grade from garnet grade in the vicinity of the Himalayan Unconformity, across kyanite-in, staurolite-in and -out, K-feldspar-in, muscovite-out and sillimanite-in isograds, up to the top of the MCTZ (Figs. 3, 7 and 12d; Appendix B; Hubbard, 1989; Meier and Hiltner, 1993; Lombardo et al., 1993; Goscombe and Hand, 2000). Only the highest structural levels, immediately below the HHT, have rare migmatitic segregations with paratactic garnet and both prismatic and fibrolitic sillimanite (Fig. 7; Appendix B). There are no sharp discontinuities within this inverted metamorphic zonation, which is characteristic of the MCTZ throughout the central Himalaya, in central Nepal (e.g. Hubbard, 1996; Vannay and Hodges, 1996; Fraser et al., 2000), Sikkim (Mohan et al., 1989; Dasgupta et al., 2004) and Bhutan (Daniel et al., 2003). In eastern Nepal, peak metamorphism ranges 550 to 650 °C across the MCTZ, at pressures averaging 8.8± 1.1 kbar and *T*/depth ratios (i.e. average thermal gradient) range 18–21 °C/km (Fig. 12e, f; Meier and Hiltner, 1993; Goscombe and Hand, 2000). Maximum pressures were attained prior to the peak-*T* of metamorphism, and average 10.0±1.2 kbar at approximately 550 °C (Goscombe and Hand, 2000).

Mineral textures preserve evidence of a complex reaction history in the MCTZ, with at least two periods of metamorphic mineral growth (e.g. Kohn et al., 2001; Appendix B). Garnets show distinct cores with typical prograde growth zoning, overgrown by post-kinematic idioblastic garnet with partially resorbed margins (Davidson et al., 1997; Goscombe and Hand, 2000; Kohn et al., 2001; Daniel et al., 2003). Sequence of mineral growth, typified by early staurolite overgrown by garnet, kyanite replaced by sillimanite and Ca-rich plagioclase rims, indicate decompression through the peak of metamorphism, and suggest broadly similar clockwise *P–T* paths in all parts of the MCTZ (Fig. 12e, f; Goscombe and Hand, 2000).

Recent geochronology of matrix metamorphic minerals (i.e. garnet, monazite and xenotime), from the Darondi and Langtang Valleys in central Nepal and Sikkim and Bhutan, are evidence for a diachronous multi-stage metamorphic history in the MCTZ. Th–Pb monazite ages from the highest structural levels, immediately below the HHT, range in age between 18 and 22 Ma (Kohn et al., 2001; Daniel et al., 2003), overlapping with the youngest metamorphic age determinations from the Upper-Plate. Down through the MCTZ, monazite ages range semi-systematically from 16–12 Ma to 8.9 Ma near the Himalayan Unconformity, immediately above the MCT as originally defined (Fig. 3; Kohn et al., 2001; Daniel et al., 2003; Catlos et al., 2004; Kohn et al., 2005).

6.3.2. Footwall below the Himalayan Unconformity

There is an increase in metamorphic grade from sub-biotite grade quartz–sericite±chlorite schists at the lowest structural levels exposed, up across the biotite-in and garnet-in isograds immediately below the MCTI (Fig. 7; Lombardo et al., 1993). Metamorphic grade varies smoothly; there is no metamorphic discontinuity at the MCT in the Ulleri Formation, nor across the Himalayan Unconformity at slightly higher structural levels (Figs. 3 and 7). Footwall schists experienced one metamorphic event evidenced by single-stage, syn-kinematic prograde garnet growth (Goscombe and Hand, 2000). Peak metamorphic conditions average 561±12 °C and 7.4±1.9 kbar with *T*/depth ratio of ~22 °C/km (Fig. 12e, f). Garnet zoning preserves the prograde burial sector of a clockwise *P–T* path with maximum pressures of 8.5 kbar (Goscombe and Hand, 2000). In central Nepal, Ar–Ar and Th–Pb monazite ages from low-grade schist in the footwall below both the Himalayan Unconformity and MCT (as originally defined) are ~8–6 Ma (Macfarlane et al., 1992; Harrison et al., 1997; Kohn et al., 2001).

7. Discussion

7.1. Upper-Plate/Lower-Plate discontinuity

The Mesoproterozoic Lesser Himalayan Sequence and overlying Neoproterozoic–Cambrian Greater Himalayan Sequence are clearly distinguished on lithostratigraphic grounds (Colchen et al., 1986), Nd isotopic compositions (Parrish and Hodges, 1996; Ahmad et al., 2000; Robinson et al., 2001; Martin et al., 2005 and references cited therein) and detrital zircon ages (DeCelle et al., 2000; Robinson et al., 2001). In eastern Nepal the Himalayan Unconformity between these two basinal sequences does not coincide with a discrete thrust or high strain zone (Fig. 3). As recognised elsewhere (Searle et al., 2002), the Himalayan Unconformity occurs within the broad MCTZ at a structural level above the MCT as originally defined (Heim and Gansser, 1939; Gansser, 1964, 1983; Fig. 4). In eastern Nepal the Himalayan Unconformity is not synonymous with either the originally defined MCT or with the major Upper-Plate/Lower-Plate discontinuity marking the top of the MCTZ. This is in contrast to the central Nepal region where the Himalayan Unconformity is mapped as coincident with the major Upper-Plate/Lower-Plate tectonic discontinuity, also named MCT in this region (i.e. Vannay and Hodges, 1996; Hodges et al., 1996; Harrison et al., 1997; Kohn et al., 2001, 2005; Fig. 4). The Himalayan Unconformity has also been mapped as coinciding with the kyanite-in isograd (e.g. LeFort, 1975; Gansser, 1983; Pêcher, 1989; Upreti and Yoshida, 2005), and though typically close, the two are coincident in only the westernmost part of eastern Nepal region investigated (Fig. 7). Confusion arising from defining the Himalayan Unconformity in association with a major tectonic structure may have arisen from an assumed correlation between the similar terms: Greater Himalayan Sequence (stratigraphic) and Greater Himalayan Zone (tectonic). Where possible, the Himalayan Unconformity must be established independently of strain and its relationship to the metamorphic architecture, and not defined interchangeably with a deformational structure.

As has been recognised throughout the central Himalaya, the Himalayan Metamorphic Front contains a marked deformation-al-metamorphic-chronologic discontinuity between inverted

amphibolite facies metamorphics and the overlying high-grade, gneissic and migmatitic High Himalayan Crystallines (Hodges, 2000; Hodges et al., 2001). In central and western Nepal and into NW India, this discontinuity has been correlated with the unconformity between the Greater Himalayan Sequence and Lesser Himalayan Sequence, occurring at the principle thrust of the inverted metamorphic sequence, and called the MCT by most workers (Fig. 4; Stöcklin, 1980; Hodges et al., 1988; Searle and Rex, 1989; Inger and Harris, 1992; Macfarlane et al., 1992; Hodges et al., 1996; Hubbard, 1996; Vannay and Hodges, 1996; Kohn et al., 2001, 2005; Pearson and DeCelles, 2005). Searle et al. (2002) recognised that the main discontinuity was above the unconformity between the Greater Himalayan Sequence and Lesser Himalayan Sequence and separated the deformational structure from the stratigraphic unconformity (Fig. 4). Our work has shown that this critical observation can be applied along strike into eastern Nepal. We feel that the Upper-Plate/Lower-Plate discontinuity must be defined independently of the Himalayan Unconformity with which it is not associated. Furthermore, the Upper-Plate/Lower-Plate discontinuity should not be confused with the name MCT, which was originally defined at a much lower structural level within the Lesser Himalayan Sequence, immediately below the Himalayan Unconformity (Heim and Gansser, 1939; Gansser, 1964, 1983).

In eastern Nepal, the HHT is a discrete, 100–400 m thick, crustal-scale shear zone with strain significantly higher than background and is the median structure marking the only major discontinuity within the Himalayan Metamorphic Front. The HHT is situated within the Greater Himalayan Sequence at high structural levels (between 2000–3400 m altitude), and does not coincide with the unconformity between the Greater Himalayan Sequence and Lesser Himalayan Sequence at structural levels 350–1900 m lower. The HHT controls the metamorphic and deformational architecture of the Himalayan Metamorphic Front, and marks the Upper-Plate/Lower-Plate boundary in eastern Nepal. This structure is apparently continuous into Sikkim through Chungthang village (Dasgupta et al., 2004; Catlos et al., 2004) and possibly links with the Kakhtang Thrust at similar structural level in Bhutan (Grujic et al., 1996; Davidson et al., 1997; Grujic et al., 2002; Daniel et al., 2003). To the west, the HHT links with the major structure at the top of the MCTZ in central and western Nepal that has previously been labelled the MCT (Figs. 2 and 4).

The key features of the boundary zone between the Upper-Plate and Lower-Plate, centred on the HHT in eastern Nepal and its lateral equivalent elsewhere are listed below, and presented in the synthesised field gradients and profile (Fig. 13).

(1) Strain variation across the Lower-Plate increases on average towards the HHT and is punctuated by discrete thrust surfaces within the MCTZ and high strain domains with strain ratios of 16–20 at the MCT. The HHT is the only thick significantly high strain structure in the Himalayan Metamorphic Front. Strain ratios of 30–45 and grain refinement of >90% of the rock by dynamic recrystallization and grain size reduction is significantly greater than background (Fig. 13). Above the HHT strain is relatively low, heterogeneously distributed and decreases upwards through the Upper-Plate until near the STDS.

(2) The HHT marks a sharp change in deformational style and textural relationships. The Lower-Plate is a broad homoclinal zone of transposed schistosity with strong stretching lineations plunging down-dip and reverse shear sense. In contrast the Upper-Plate has complex internal geometry, multiple migmatite generations, coarse-grained, differentiated gneissic fabrics, bimodal stretching lineation directions and shear bands with reverse and normal shear sense. These marked differences in deformational style reflect contrasting mechanical properties between the two levels of the orogen, the rheology being primarily influenced by significantly different metamorphic conditions in the two levels (see below).

(3) Metamorphic zonation varies smoothly across most of the Himalayan Metamorphic Front, with the exception of a rapid transition centred on the HHT (Figs. 12e, f and 13). The inverted moderate-*T*/high-*P* (18–22 °C/km) sequence in the Lower-Plate contrasts strongly with high-grade migmatite-rich metamorphic rocks in the Upper-Plate. The Upper-Plate is of high-*T*/moderate-*P* type (30–40 °C/km) with temperatures up to 190 °C higher, and pressures 2 kbar lower than the Lower-Plate (Fig. 12e and f; Goscombe and Hand, 2000). Steep advection-dominated clockwise paths in the Lower-Plate contrast with conduction-dominated metamorphism terminated by near isobaric cooling in the Upper-Plate (Fig. 12b, c; Goscombe and Hand, 2000). Characteristic metamorphic conditions of the Lower- and Upper-Plates are separated by a transitional zone, centred on the HHT and in part, indicating continuation of the inverted metamorphic zonation (Figs. 7, 12e, f and 13). The HHT marks the upper-limit of muscovite and fibrolite and lower-limit of cordierite in all traverses, and the lower-limit of migmatization in most traverses east of the Arun River (Fig. 7; Appendix B). In the Everest–Makalu region, kyanite persists up into lowermost Upper-Plate (Lombardo et al., 1993), but is absent east of the Arun River suggesting a sharper metamorphic discontinuity (Fig. 7; Appendix B). The contrasting metamorphic styles of the Upper- and Lower-Plates suggest the cause of metamorphism was different and operating somewhat independently either side of the HHT. High temperatures and *T*/depth ratios in the Upper-Plate are probably due to rapid exhumation, driven by extrusion, of hot rocks into shallower crustal levels (Grujic et al., 1996; Davidson et al., 1997; Beaumont et al., 2001; Jamieson et al., 2004), in contrast to crustal over-thickening and conductively driven regimes in the Lower-Plate (Jamieson et al., 1996).

(4) The HHT is central to a transition zone in the age distribution of main phase deformation and peak metamorphism. The entire Upper-Plate experienced peak metamorphism at ~22–24 Ma. Metamorphism was younger and diachronous across the Lower-Plate, with younger events at lower

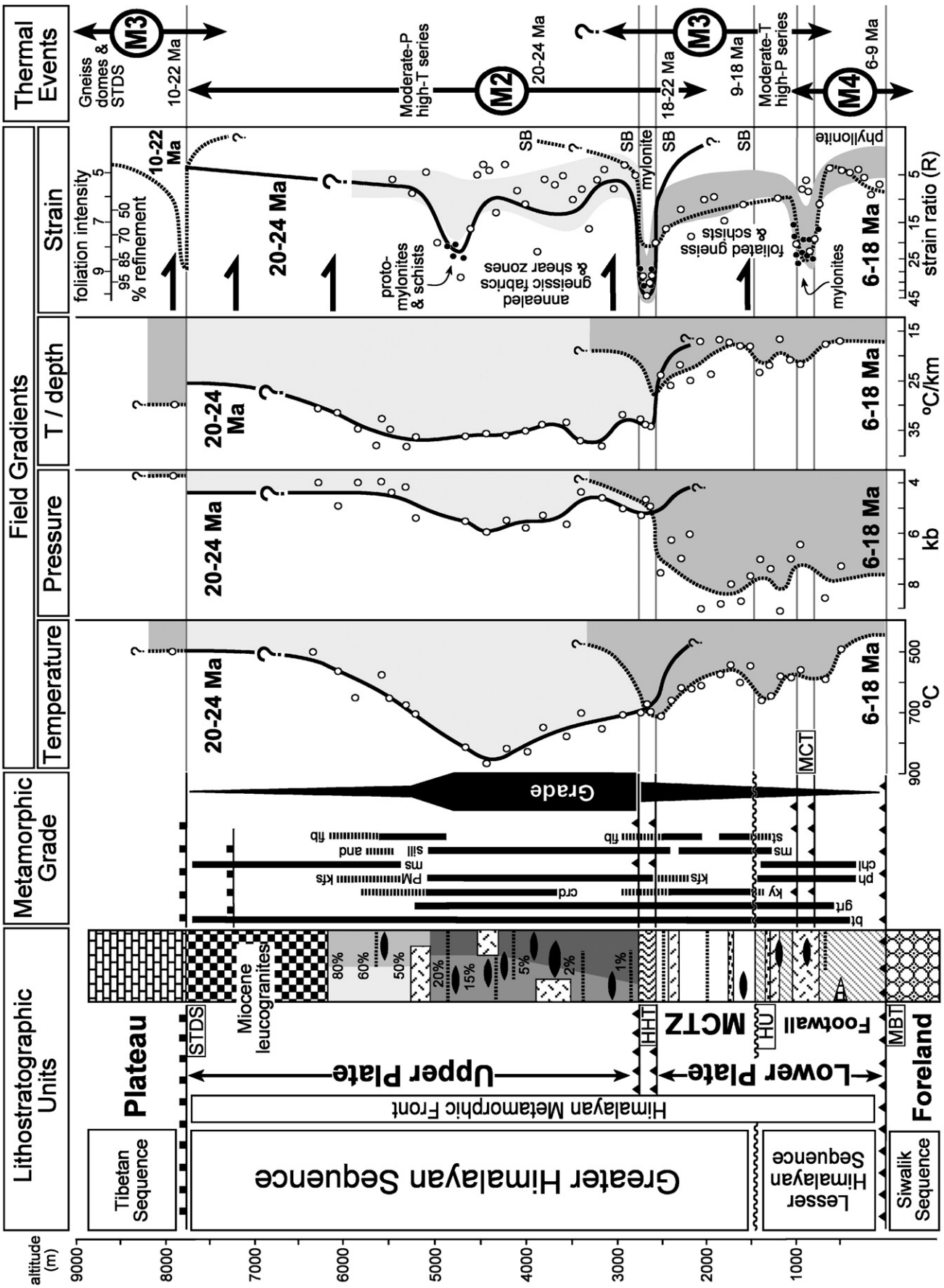
Thermal Events
Field Gradients
Metamorphic Grade
Lithostratographic Units
Strain
T / depth
Pressure
Temperature
Gneiss domes & STDS
M3
10-22 Ma
Moderate-P high-T series
M2
20-24 Ma
18-22 Ma
9-18 Ma
Moderate-T high-P series
M4
6-9 Ma
foliation intensity
% refinement
strain ratio (R)
proto-mylonites & schists
annealed gneissic fabrics & shear zones
mylonite
folated gneiss & schists
phyllonite
mylonites
SB
°C/km
kb
°C
Grade
MCT
STDS
HHT
HT
MBT
Miocene leucogranites
Plateau
Upper Plate
Lower Plate
MCTZ
Footwall
Foreland
Himalayan Metamorphic Front
Greater Himalayan Sequence
Lesser Himalayan Sequence
Tibetan Sequence
Siwalik Sequence
altitude (m)

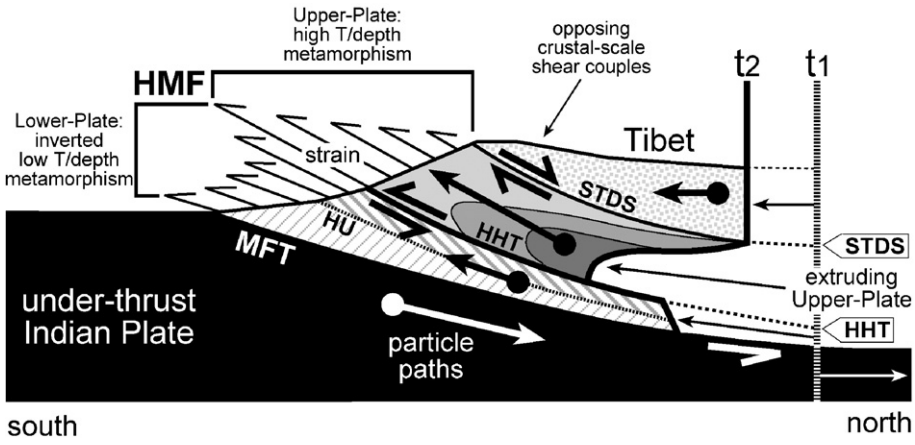

Fig. 14. Diagrammatic section through the Himalayan Metamorphic Front modified after Grujic et al. (1996) and Beaumont et al. (2001), with strain gradient, particle paths and general shear sense couples superimposed. The main structural and metamorphic discontinuity controlling orogen architecture, and defining the Upper-Plate/Lower-Plate boundary, is the High Himal Thrust (HHT), not the unconformity between the Lesser- and Greater Himalayan Sequences at lower structural levels (dashed line between different shadings). Note that the STDS is a normal fault formed in an overall contractional system. The central Himalayan Orogen has been convergent for at least the last 30 Ma and all domains above the Main Frontal Thrust have been transported south relative to the underthrust Indian Plate throughout this time. The Upper-Plate portion of the Himalayan Metamorphic Front has been transported southwards by extrusion, at a faster rate than both the adjacent Lower-Plate below the HHT and the Tibetan Sequence above the STDS.

structural levels (e.g. Harrison et al., 1997); metamorphism at 18–22 Ma immediately below the HHT, 16–12 Ma in the central MCTZ, 8–9 Ma immediately above the MCT (as originally defined) and 8–6 Ma below the MCT (Fig. 3). Younger metamorphic events in the Lower-Plate did not pervasively metamorphose or rework the overlying Upper-Plate.

7.2. Extrusional telescoping of the Himalayan Metamorphic Front

The 4300–6000 m thick Upper-Plate extruded upward and southward during main phase deformation and metamorphism from ~24 to 20 Ma (Fig 14; Grujic et al., 1996; Davidson et al., 1997; Hodges et al., 2001; Beaumont et al., 2001; Grujic et al., 2002; Jamieson et al., 2004). Upper-Plate extrusion was accommodated by both; (1) reverse shear deformation distributed pervasively throughout the internal body of the Upper-Plate and enhanced by both the ductile high-grade metamorphic conditions and relatively high proportion of melt as indicated by preserved migmatitic leucosomes (Harris and Massey, 1994; Gaillard et al., 2004), and (2) the gross-scale shear couple of bounding crustal-scale structures of opposing relative shear sense (Fig. 14; Beaumont et al., 2001; Grujic et al., 2002; Jamieson et al., 2004). The lower bounding structure is the reverse HHT and normal movements in the STDS mark the upper boundary of the Upper-Plate (Burg et al., 1984; Burchfiel et al., 1992), both broadly active between 22 and 11 Ma (Searle, 1999; Harrison et al., 1999; Godin et al., 2001; Catlos et al., 2004). Initiation of movement in the HHT was possibly as young as 16 Ma (Harris et al., 2004; Kohn et al., 2005) and continued to at least 13 Ma (Daniel et al., 2003). Material was extruded along vectors approximating stretching lineations, parallel to orogen-scale tectonic transport defined by seafloor spreading histories (Shackleton and Ries, 1984; Grujic et al., 2002). The high exhumation rates accompanying extrusion of the Upper-Plate was driven by gravity, due to the pressure difference between the over-thickened orogen interior and normal crust of the foreland, and accommodated by high erosion rates in the Himalayan Metamorphic Front (e.g. Beaumont et al., 2001; Jamieson et al., 2004; Vannay et al., 2004; Thiede et al., 2005).

Unresolved in the Himalayan Metamorphic Front is the origin of high-*T*/depth ratios and low pressures in the Upper-Plate with respect to the Lower-Plate, this being incompatible with reverse transport of the Upper-Plate from deeper crustal levels over higher-pressure and younger rocks in the Lower-Plate. There are two alternative explanations; either (1) a high pressure early metamorphic history in the Upper-Plate has not been recognised/preserved, or (2) the Himalayan Metamorphic Front was further telescoped by a later phase of Lower-Plate extrusion akin to that experienced by the Upper-Plate. An early high-pressure history may have been obliterated by high

Fig. 13. Generalized section across the Himalayan Metamorphic Front based on the average of the eight profiles documented (Fig. 7). Sections represent rock units, major structures, diagnostic mineral parageneses (Appendix A) and metamorphic grade. Legend is the same as in Fig. 7. Smoothed field gradients are superimposed on strain and metamorphic data from throughout eastern Nepal. Published *P–T* calculations (circles) are from east of Mount Everest (Pognante and Benna, 1993; Goscombe and Hand, 2002; Appendix B; Fig. 12). Semi-quantitative strain ratio (circles), degree of grain refinement (dots) and qualitative foliation intensity (shaded) data are listed in Appendix A and located in Figs. 8 and 11. Strain markers and metamorphic parageneses are not time equivalent across the Himalayan Metamorphic Front. Thus different portions of field gradients have been correlated with age constraints from throughout the central Himalaya (e.g. Harrison et al., 1997; Simpson et al., 2000; Kohn et al., 2001). Solid line and pale shading—main phase 20–24 Ma events in Upper-Plate. Dashed line and dark shading—main phase 6–18 Ma events in Lower-Plate. Note that both metamorphism and deformation propagated southward with time (Fig. 5). Almost all deformation is associated with reverse shear, except for extensional, top down to the north shear at structural levels indicated by half arrows. SB—late-stage shear bands and shear zones are present.

temperatures in the Upper-Plate facilitating continuing reequilibration during rapid extrusion and late closure of metamorphic parageneses at relatively low pressures. Further telescoping of the Himalayan Metamorphic Front by late-stage Lower-Plate extrusion relative to the Upper-Plate would bring the younger (18–6 Ma) and deeper Lower-Plate rocks up into juxtaposition with older (24–20 Ma) and shallower Upper-Plate rocks. This model of ongoing telescoping of the Himalayan Metamorphic Front implies a southward propagation of the extruding "wedge" over time with successively older hanging walls: initially the Upper-Plate from ~24 Ma and possibly multiple periods in the Lower-Plate between 18 and 6 Ma (Fig. 13).

There is some evidence for ongoing telescoping of the Himalayan Metamorphic Front. Some form of differential exhumation is required to bring the deeper but younger (18–6 Ma) Lower-Plate metamorphics into juxtaposition with older (24–20 Ma) Upper-Plate metamorphics. Diachronous metamorphism across the Himalayan Metamorphic Front, and progressively younger ages down through the Lower-Plate, imply late-stage thrusting of Lower-Plate rocks along structures at low structural levels, such as in the vicinity of the MCT (as originally defined), as has been recognised by Harrison et al. (1997) and Kohn et al. (2001, 2005). Late-stage Lower-Plate extrusion would require structural accommodation by extensional reactivation at high structural levels such as at the HHT or surfaces within the Lower-Plate. In the vicinity of the HHT, there is evidence for lower-grade, late-stage reactivation and top down to the north, normal shear bands (Figs. 8 and 13), and there is evidence for top down to the north, normal reactivation of the main foliation immediately above the Himalayan Unconformity (Fig. 8 and 13; Appendix A). Consequently, in addition to Upper-Plate extrusion, two speculative periods of extrusion-like, transport of domains within the Lower-Plate can be proposed, continuing the long-term southward propagation of the active orogenic front (Fig. 5). (1) Extrusion of the MCTZ domain between ~18 and 9 Ma, accommodated by thrusting on the MCT (as originally defined) and top down to the north, normal reactivation in the vicinity of the HHT. (2) Extrusion of the footwall domain (Fig. 3) at <9 Ma, accommodated by thrusting on the Main Boundary Thrust and top down to the north, normal reactivation of the main foliation immediately above the Himalayan Unconformity. High rates of erosion-controlled exhumation at this same structural level, since the Miocene, have been reported in NW India (Vannay and Grasemann, 2001; Vannay et al., 2004; Thiede et al., 2005).

8. Conclusions

Mapping has shown Himalayan Metamorphic Front architecture is not fundamentally controlled by the MCT (as originally defined). In eastern Nepal, no significant deformational structure is recognised at the Himalayan Unconformity, between Mesoproterozoic Lesser Himalayan Sequence and the overlying Neoproterozoic Greater Himalayan Sequence. The unconformity is marked by an abrupt change in rock types between two equally deformed basinal sequences. It cannot be viewed as a fundamental crustal structure controlling evolution of the Himalayan Metamorphic Front. In eastern Nepal, Sikkim and Bhutan the main structural discontinuity, marking the Upper-Plate/Lower-Plate boundary in the Himalayan Metamorphic Front, is a zone of high-strain defined as the HHT. The HHT is sited within the Greater Himalayan Sequence, and does not coincide with the unconformity between the Greater Himalayan Sequence and Lesser Himalayan Sequence. In central and western Nepal this is different; the Upper-Plate/Lower-Plate boundary is called the MCT and it is in the vicinity of the unconformity between the Greater- and Lesser Himalayan Sequences. Nevertheless, the Upper-Plate/Lower-Plate boundary is continuous between both regions and throughout is a crustal-scale high strain shear zone marking a major discontinuity in strain and deformation style. It is the median structure within a rapid transition in metamorphic style and timing of main phase deformation and metamorphism. This Upper-Plate/Lower-Plate discontinuity is the orogen-median structure that controlled the evolution and metamorphic structure of the Himalayan Metamorphic Front and governs erosion controlled and differential pressure driven southward extrusion of mid-crustal rocks from under the Tibetan Plateau.

Along-orogen variation in the stratigraphic and structural level of the Upper-Plate/Lower-Plate boundary indicates that fundamental architecture of the Himalayan Metamorphic Front varies along the length of the Himalayan Orogen. Thickness of Greater Himalayan Sequence within the MCTZ increases from central Nepal and across eastern Nepal (Fig. 7) to Sikkim and Bhutan (Figs. 1 and 2). Furthermore, the thickness of the Upper-Plate increases from 1000–2000 m in central Nepal (Pêcher, 1989; Vannay and Hodges, 1996; Hodges et al., 1996) to 4300–6000 m in eastern Nepal (Fig. 7). This change in architecture of the Himalayan Metamorphic Front starts at approximately the longitude of Mount Everest and Upper-Plate and Greater Himalayan Sequence thicknesses gradually increase across the eastern Nepal Region ((Figs. 1, 2 and 7)). This lateral change may ultimately be due to either ad hoc second order variations within a large and complex orogenic system, or alternatively be due to systematic change in first order variables such as erosion rates (and rainfall) at the orogen front, crustal strength, crustal thickness, distribution of heat-producing radiogenic elements, or crustal plate geometry (e.g. Brown and Solar, 1999; Beaumont et al., 2001; Jamieson et al., 2004).

Acknowledgements

This research was supported by ARC Large Grant A00103456, awarded to DRG, two Adelaide University Small Grants awarded to BG and MH, Adelaide University Start up Grant awarded to MH and private funds (BG). Research was undertaken while BG was an Honorary Research Fellow at Adelaide University and supported as a Post-Doctoral Fellow of ARC Large Grant A00103456. Write-up was undertaken while BG was on leave from the NT Geological Survey. BG acknowledges support from the Adelaide University and the University of Melbourne. Permission to undertake research in Nepal was sponsored by Prof. B.N. Upreti at Tribhuvan University for which we are grateful. Fieldwork was facilitated

by the hard work and generosity of numerous people, including Prem and Hem Aburami, Pashi-Aundi Sherpa, Suresh Shrestha, Kancha Lama, Ram Lama, Phaum Bardo Lama, Aasha Sherpa, Pudum Tamang, Baijaya Tamang, Babu Tamang, Chuwong Tamang and Choisang Lama. We acknowledge discussions on Himalayan geology with Bishal Upreti, Kurt Stuwe, Mike Sandiford and the late Robin Oliver who inspired this research project. Nd isotopic analyses was undertaken by Karin Barovich and Ben Wade. The reviews of B. Grasemann and D. Grujic are gratefully acknowledged for their significant improvement to the manuscript.

Appendix A. Supplementary materials

Supplementary data associated with this article can be found, in the online version, at doi:10.1016/j.gr.2006.05.003.

References

Ahmad, T., Harris, N., Bickle, M., Chapman, H., Bunbury, J., Prince, C., 2000. Isotopic constraints on the structural relationships between the Lesser Himalayan Series and the High Himalayan Crystalline Series, Garhwal Himalaya. Geological Society of America Bulletin 112, 467–477.

Arita, K., 1983. Origin of the inverted metamorphism of the Lower Himalayas central Nepal. Tectonophysics 95, 43–60.

Arita, K., Ganzawa, Y., 1997. Thrust tectonics and uplift process of the Nepal Himalaya revealed from fission-track ages. Journal of Geography 106, 156–167.

Beaumont, C., Jamieson, R.A., Nguyen, M.H., Lee, B., 2001. Himalayan tectonics explained by extrusion of a low-viscosity crustal channel coupled to focused surface denudation. Nature 414, 738–742.

Bordet, P., 1961. Recherches Geologiques Dans l'Himalaya du Nepal, Region du Makalu. Editions du Centre National Recherches Scientifiques, Paris.

Brown, M., Solar, G.S., 1999. The mechanism of ascent and emplacement of granite magma during transpression; a syntectonic granite paradigm. Tectonophysics 312, 1–33.

Brunel, M., Kienast, J.-R., 1986. Etude petro-structurale des chevauchements ductiles himalayens sur la transversale de l'Everset-Makalu (Nepal oriental). Canadian Journal of Earth Science 23, 1117–1137.

Burchfiel, B.C., Zhiliang, C., Hodges, K.V., Yuping, L., Royden, L.H., Changrong, D., Jiene, X., 1992. The South Tibetan Detachment System, Himalayan Orogen: Extension contemporaneous with and parallel to shortening in a collisional mountain belt. Geological Society of America, Special Paper 269, 41.

Burg, J.P., Guiraud, M., Chen, G.M., Li, G.C., 1984. Himalayan metamorphism and deformations in the North Himalayan Belt (southern Tibet, China). Earth and Planetary Science Letters 69, 391–400.

Catlos, E.J., Dubey, C.S., Harrison, T.M., Edwards, M.A., 2004. Late Miocene movement within the Himalayan Main Central Thrust shear zone, Sikkim, north-east India. Journal of Metamorphic Geology 22, 207–226.

Colchen, M., LeFort, P., Pêcher, A., 1986. Recherches geologiques dans l'Himalaya du Nepal Annapurna Manaslu, Ganesh. Paris Editions du Centre National de la Recherche Scientifique, Paris, p. 136.

Coleman, M.E., 1998. U–Pb constraints on Oligocene–Miocene deformation and anatexis within the central Hmalaya, Marsyandi Valley, Nepal. American Journal of Science 298, 553–571.

Daniel, C.G., Hollister, L.S., Parrish, R.R., Grujic, D., 2003. Exhumation of the Main Central Thrust from Lower Crustal Depths, Eastern Bhutan Himalaya. Journal of Metamorphic Geology 21, 317–334.

Dasgupta, S., Ganguly, J., Neogi, S., 2004. Inverted metamorphic sequence in the Sikkim Himalayas: crystallization history, *P–T* gradient and implications. Journal of Metamorphic Geology 22, 395–412.

Davidson, C., Grujic, D.E., Hollister, L.S., Schmid, S.M., 1997. Metamorphic reactions related to decompression and synkinematic intrusion of leucogranite, High Himalayan Crystallines, Bhutan. Journal of Metamorphic Geology 15, 593–612.

DeCelles, P.G., Gehrels, G.E, Quade, J., Ojha, T.P., Kapp, P.A., Upreti, B.N., 1998. Neogene foreland basin deposits erosional unroofing and the kinematic history of the Himalayan fold-thrust belt, western Nepal. Geological Society of America Bulletin 110, 2–21.

DeCelle, P.G., Gehrels, G.E., Quade, J., Lareau, B., Spurlin, M., 2000. Tectonic implications of U–Pb zircon ages of the Himalayan Orogenic Belt in Nepal. Science 288, 497–499.

Dewey, J.F., Cande, S., Pitman III, W.C., 1989. Tectonic evolution of the India/Eurasia collision zone. Eclogae Geologicae Helvetiae 82/3, 717–734.

Edwards, M.A., Harrison, T.M., 1997. When did the roof collapse? Late Miocene north–south extension in the high Himalaya revealed by Th–Pb monazite dating of the Khula Kangri granite. Geology 25, 543–546.

Fraser, G., Worley, B., Sandiford, M., 2000. High-precision geothermobarometry across the High Himalayan metamorphic sequence, Langtang Valley, Nepal. Journal of Metamorphic Geology 18, 665–681.

Gaillard, F., Scaillet, B., Pichavant, M., 2004. Evidence for present-day leucogranite pluton growth in Tibet. Geology 32, 801–804.

Gansser, A., 1964. Geology of the Himalayas. Wiley Interscience, London, p. 289.

Gansser, A., 1983. Geology of the Bhutan Himalaya. Birkhäuer Verlag, Basel, p. 181.

Godin, L., Brown, R.L., Hanmer, S., 1999. High strain zone in the hanging wall of the Annapurna detachment, central Nepal Himalaya. In: Macfarlane, A., Sorkhabi, R.B., Quade, J. (Eds.), Himalaya and Tibet: Mountain Roots to Mountain Tops. Geological Society of America Special Paper, vol. 328, pp. 199–210.

Godin, L., Parrish, R.R., Brown, R.L., Hodges, K.V., 2001. Crustal thickening leading to exhumation of the Himalayan metamorphic core of central Nepal: Insight from U–Pb geochronology and $^{40}Ar/^{39}Ar$ thermochronology. Tectonics 20, 729–747.

Goscombe, B.D., Hand, M., 2000. Contrasting *P–T* paths in the Eastern Himalaya, Nepal: inverted isograds in a Paired Metamorphic Mountain Belt. Journal of Petrology 41, 1673–1719.

Goscombe, B., Hand, M., 2002. What is the Main Central Thrust of the Himalayan Orogen? 16th Australian Geological Convention Geological Society of Australia, Abstracts.

Goscombe, B., Hand, M., Gray, D., 2003. Structural and metamorphic architecture of the east Nepal Himalayas. Specialist Group in Tectonics and Structural Geology, Kalbarri. Geological Society of Australia. Abstracts.

Goscombe, B.D., Passchier, C.W., Hand, M., 2004. Boudinage classification: end-member boudin types and modified boudin structures. Journal of Structural Geology 26, 739–763.

Grujic, D., Casey, M., Davidson, C., Hollister, L.S., Kundig, R., Pavlis, T., Schmid, S., 1996. Ductile extrusion of the Higher Himalayan crystalline in Bhutan: evidence from quartz microfabrics. Tectonophysics 260, 21–43.

Grujic, D., Hollister, L.S., Parrish, R.R., 2002. Himalayan metamorphic sequence as an orogenic channel: insight from Bhutan. Earth and Planetary Science Letters 198, 177–191.

Harris, N., Massey, J., 1994. Decompression and anatexis of Himalayan metapelites. Tectonics 13, 1537–1546.

Harris, N.B.W., Caddick, M., Kosler, J., Goswami, S., Vance, D., Tindle, A.G., 2004. The pressure–temperature–time path of migmatites from Sikkim Himalaya. Journal of Metamorphic Geology 22, 249–264.

Harrison, T.M., Ryerson, F.J., LeFort, P., Yin, A., Lovera, O.M., Catlos, E.J., 1997. A Late Miocene–Pliocene origin for the Central Himalayan inverted metamorphism. Earth and Planetary Science Letters 146, E1–E7.

Harrison, T.M., Grove, M., McKeegan, K.D., Coath, C.D., Lovera, O.M., LeFort, P., 1999. Origin and episodic emplacement of the Manaslu Intrusive Complex, Central Himalaya. Journal of Petrology 40, 3–19.

Hashimoto, S., Ohta, Y., Akiba, C., 1973. Geology of the Nepal Himalayas. Saikon, Tokyo.

Heim, A., Gansser, A., 1939. Central Himalaya: geological observations of the Swiss expedition 1936. Memior Society Helvettica Science Nature 73, 1–245.

Hobbs, B.E., Means, W.D., Williams, P.F., 1983. An Outline of Structural Geology. John Wiley, New York, p. 571.

Hodges, K.V., 2000. Tectonics of the Himalaya and southern Tibet from two perspectives. Geological Society of America Bulletin 112, 324–350.

Hodges, K.V., Hubbard, M.S., Silverberg, D.S., 1988. Metamorphic constraints on the thermal evolution of the thermal evolution of the central Himalayan Orogen. Philosophical Transactions of the Royal Society of London. A 326, 257–280.

Hodges, K.V., Parrish, R.R., Searle, M.P., 1996. Tectonic evolution of the central Annapurna Range, Nepalese Himalayas. Tectonics 15, 1264–1291.

Hodges, K., Bowring, S., Davidek, K., Hawkins, D., Krol, M., 1998. Evidence for rapid displacement on Himalayan normal faults and the importance of tectonic denudation in the evolution of mountain ranges. Geology 26, 483–486.

Hodges, K.V., Hurtado, J.M., Whipple, K.X., 2001. Southward extrusion of Tibetan crust and its effect on Himalayan tectonics. Tectonics 20, 799–809.

Hubbard, M.S., 1989. Thermobarometric constraints on the thermal history of the Main Central Thrust Zone and Tibetan Slab, eastern Nepal Himalaya. Journal of Metamorphic Geology 7, 19–30.

Hubbard, M.S., 1996. Ductile shear as a cause of inverted metamorphism: example from the Nepal Himalaya. Journal of Geology 104, 493–499.

Hubbard, M.S., Harrison, T.M., 1989. $^{40}Ar/^{39}Ar$ age constraints on deformation and metamorphism in the Main Central Thrust Zone and Tibetan Slab, eastern Nepal Himalaya. Tectonics 8, 865–880.

Huyghe, P., Galy, A., Mugnier, J.-L., France-Lanord, C., 2001. Propagation of the thrust system and erosion in the Lesser Himalaya: Geochemical and sedimentological evidence. Geology 29, 1007–1010.

Inger, S., Harris, N.B.W., 1992. Tectonothermal evolution of the High Himalayan Crystalline Sequence, Langtang Valley, northern Nepal. Journal of Metamorphic Geology 10, 439–452.

Jamieson, R.A., Beumont, C., Hamilton, J., Fullsack, P., 1996. Tectonic assembly of inverted metamorphic sequences. Geology 24, 839–842.

Jamieson, R.A., Beaumont, C., Medvedev, S., Nguyen, M.H., 2004. Crustal channel flows: 2. Numerical models with implications for metamorphism in the Himalayan–Tibetan orogen. Journal of Geophysical Research 109, B06407.

Kohn, M.J., Catlos, E.J., Ryerson, F.J., Harrison, T.M., 2001. Pressure–temperature–time path discontinuity in the Main Central thrust zone, central Nepal. Geology 29, 571–574.

Kohn, M.J., Wieland, M.S., Parkinson, C.D., Upreti, B.N., 2005. Five generations of monazite in Langtang gneisses: implications for chronology of the Himalayan metamorphic core. Journal of Metamorphic Geology 23, 399–406.

Kretz, R., 1983. Symbols for rock-forming minerals. American Mineralogist 68, 277–279.

Law, R.D., Searle, M.P., Simpson, R.L., 2004. Strain, deformation temperatures and vorticity of flow at the top of the Greater Himalayan Slab, Everest Massif, Tibet. Journal of the Geological Society, London 161, 305–320.

Leech, M.L., Singh, S., Jain, A.K., Klemperer, S.L., Manickavasagam, R.M., 2005. The onset of India–Asia continental collision: early, steep subduction required by the timing of UHP metamorphism in the western Himalaya. Earth and Planetary Science Letters 234, 83–97.

LeFort, P., 1975. Himalayas: the collided range. Present knowledge of the continental arc. American Journal of Science 275, 1–44.

LePichon, X., Fournier, M., Jolivet, L., 1992. Kinematics, topography, shortening, and extrusion in the India–Eurasia collision. Tectonics 11, 1085–1098.

Lombardo, B., Pertusati, P., Borghi, S., 1993. Geology and tectonomagmatic evolution of the eastern Himalaya along the Chomolunga-Makalu transect. In: Treloar, P.J., Searle, M.P. (Eds.), Himalayan Tectonics. Geological Society Special Publication, vol. 74, pp. 323–340.

Macfarlane, A.M., 1995. An evaluation of the inverted metamorphic gradient at Langtang National Park, Central Nepal Himalaya. Journal of Metamorphic Geology 13, 595–612.

Macfarlane, A.M., Hodges, K.V., Lux, D., 1992. A structural analysis of the Main Central thrust zone, Langtang National Park, central Nepal Himalaya. Geological Society of America Bulletin 104, 1389–1402.

Maluski, H., Matte, P., Brunel, M., 1988. Argon39–argon40 dating of metamorphic and plutonic events in the North and High Himalaya belts (southern Tibet–China). Tectonics 7, 299–326.

Martin, A.J., DeCelles, P.G., Gehrels, G.E., Patchett, P.J., 2005. Isotopic and structural constraints on the location of the Main Central Thrust in the Annapurna Range, central Nepal Himalaya. Geological Society of America Bulletin 117, 926–944.

Meier, K., Hiltner, E., 1993. Deformation and metamorphism within the Main Central Thrust zone, Arun Tectonic Window, eastern Nepal. In: Treloar, P.J., Searle, M.P. (Eds.), Himalayan Tectonics. Geological Society Special Publication, vol. 74, pp. 511–523.

Miller, C., Klötzli, U., Frank, W., Thöni, M., Grasemann, B., 2000. Proterozoic crustal evolution in the NW Himalaya (India) as recorded by circa 1.80 Ga mafic and 1.84 Ga granitic magmatism. Precambrian Research 103, 191–206.

Mohan, A., Windley, B.F., Searle, M.P., 1989. Geothermobarometry and the development of inverted metamorphism in the Darjeeling-Sikkim region of the eastern Himalaya. Journal of Metamorphic Geology 7, 95–110.

Murphy, M.A., Harrison, T.M., 1999. Relationship between leucogranites and the Qomolangma detachment in the Rongbuk Valley, south Tibet. Geology 27, 831–834.

Najman, Y., Carter, A., Oliver, G., Garzanti, E., 2005. Provenance of Eocene foreland basin sediments, Nepal: constraints to the timing and diachroneity of early Himalayan orogenesis. Geology 33, 309–312.

Neogi, S., Dasgupta, S., Fukuoka, M., 1998. High-*P*–*T* polymetamorphism, dehydration melting, and generation of migmatites and granites in the Higher Himalayan Crystalline Complex, Sikkim, India. Journal of Petrology 39, 61–99.

Parrish, R.R., Hodges, K.V., 1996. Isotopic constraints on the age and provenance of the Lesser and Greater Himalayan sequences, Nepalese Himalaya. Geological Society of America Bulletin 108, 904–911.

Patriat, P., Achache, J., 1984. The chronology of the India–Eurasia collision. Implications for crustal shortening and the driving mechanism of plates. Nature 311, 615–621.

Pearson, O.N., DeCelles, P.G., 2005. Structural geology and regional tectonic significance of the Ramgarh thrust, Himalayan fold-thrust belt of Nepal. Tectonics 24, TC4008.

Pêcher, A., 1989. The metamorphism in the Central Himalaya. Journal of Metamorphic Geology 7, 31–41.

Pognante, U., Benna, P., 1993. Metamorphic zonation, migmatization and leucogranites along the Everest transect of Eastern Nepal and Tibet: record of an exhumation history. In: Treloar, P.J., Searle, M.P. (Eds.), Himalayan Tectonics. Geological Society Special Publication, vol. 74, pp. 323–340.

Ramsay, J.G., 1967. Folding and Fracturing of Rocks. Mc Graw and Hill, New York.

Ramsay, J.G., Graham, R.H., 1970. Strain variation in shear belts. Canadian Journal of Earth Sciences 7, 786–813.

Robinson, D.M., DeCelles, P.G., Garzione, C.N., Pearson, O.N., Harrison, T.M., Catlos, E.J., 2001. The kinematic evolution of the Nepalese Himalaya interpreted from Nd isotopes. Earth and Planetary Science Letters 192, 507–521.

Robinson, D.M., DeCelles, P.G., Patchett, P.J., Garzione, C.N., 2003. Kinematic model for the Main Central thrust in Nepal. Geology 31, 359–362.

Schelling, D., 1992. The tectonostratigraphy and structure of the eastern Nepal Himalaya. Tectonics 11, 925–943.

Schmid, D.W., Podladchikov, Y.Y., 2004. Are isolated stable rigid clasts in shear zones equivalent to voids? Tectonophysics 384, 233–242.

Schwab, M., Ratschbacher, L., Siebel, W., McWilliams, M., Minaev, V., Lutkov, V., Chen, F., Stanek, K., Nelson, B., Frisch, W., Wooden, J.L., 2004. Assembly of the Pamirs: age and origin of magmatic belts from the southern Tien Shan to the southern Pamirs and their relation to Tibet. Tectonics 23, TC4002.

Searle, M.P., 1999. Extensional and compressional faults in the Everest–Lhotse massif, Khumbu Himalaya, Nepal. Journal of the Geological Society, London 156, 227–240.

Searle, M.P., Godin, L., 2003. The South Tibetan detachment and the Manaslu Leucogranite; a structural reinterpretation and restoration of the Annapurna–Manaslu Himalaya, Nepal. Journal of Geology 111, 505–523.

Searle, M.P., Rex, A.J., 1989. Thermal model for the Zanskar Himalaya. Journal of Metamorphic Geology 7, 127–134.

Searle, M.P., Szulc, A.G., 2005. Channel flow and ductile extrusion of the high Himalayan slab-Kangchenjunga-Darjeeling profile, Sikkim Himalaya. Journal of Asian Earth Sciences 25, 173–185.

Searle, M.P., Waters, D.J., Stephenson, B.J., 2002. Pressure–temperature–time path discontinuity in the Main Central thrust zone, central Nepal: comment and reply. Geology 30, 479–480.

Searle, M.P., Simpson, R.L., Law, R.D., Parrish, R.R., Waters, D.J., 2003. The structural geometry, metamorphic and magmatic evolution of the Everest Massif, High Himalaya of Nepal–South Tibet. Journal of the Geological Society of London 160, 345–366.

Shackleton, R.M., Ries, A.C., 1984. The relation between regionally consistent stretching lineations and plate motions. Journal of Structural Geology 6, 111–117.

Shrestha, S.B., Shrestha, J.N., Sharma, S.R., 1984. Geological map of Eastern Nepal, 1:250,000. Ministry of Industry, Department of Mines and Geology, Lainchour, Kathmandu.

Simpson, R.L., Parrish, R.R., Searle, M.P., Waters, D.J., 2000. Two episodes of monazite crystallization during metamorphism and crustal melting in the Everest region of the Nepalese Himalaya. Geology 28 (5), 403–406.

Smythe, F.S., 1930. The Kangchenjunga Adventure. Hodder and Stoughton Ltd., London.

Stephenson, B.J., Searle, M.P., Waters, D.J., Rex, D.C., 2001. Structure of the Main Central Thrust zone and extrusion of the High Himalayan deep crustal wedge. Journal Geological Society, London 158, 637–652.

Stöcklin, J., 1980. Geology of Nepal and its regional frame. Journal of the Geological Society, London 137, 1–34.

Swapp, S.M., Hollister, L.S., 1991. Inverted metamorphism within the Tibetan slab of Bhutan: evidence for a tectonically transported heat-source. Canadian Mineralogist 29, 1019–1041.

Tapponier, P., Peltzer, G., LeDain, A.Y., Armijo, R., 1982. Propagating extrusion tectonics in Asia: new insights from simple experiments with plasticine. Geology 10, 611–616.

Tapponier, P., Peltzer, G., Armijo, R., 1986. On the mechanics of the collision between India and Asia. Geological Society of London Special Publication 19, 115–157.

Thiede, R.C., Arrowsmith, J.R., Bookhagen, B., McWilliams, M.O., Sobel, E.R., Strecker, M.R., 2005. From tectonically to erosionally controlled development of the Himalayan Orogen. Geology 33, 689–692.

Upreti, B.N., 1999. An overview of the stratigraphy and tectonics of the Nepal Himalaya. Journal of Asian Earth Sciences 17, 577–606.

Upreti, B.N., Yoshida, M., 2005. Basement history and provenance of the Tethys sediments of the Himalaya: an appraisal based on recent geochronologic and tectonic data. Abstract, Cairo Conference.

Valdiya, K.S., 1980. The two intracrustal boundary thrusts of the Himalaya. Tectonophysics 66, 323–348.

Vannay, J.-C., Hodges, K.V., 1996. Tectonometamorphic evolution of the Himalayan metamorphic core between the Annapurna and Dhaulagiri, central Nepal. Journal of Metamorphic Geology 14, 635–656.

Vannay, J.-C., Grasemann, B., 2001. Himalayan inverted metamorphism and synconvergence extension as a consequence of a general shear extrusion. Geological Magazine 138, 253–276.

Vannay, J.-C., Grasemann, B., Rahn, M., Frank, W., Carter, A., Baudraz, V., Cosca, M., 2004. Miocene to Holocene exhumation of metamorphic crustal wedges in the NW Himalaya: evidence for tectonic extrusion coupled to fluvial erosion. Tectonics 23, TC1014.

Viskupic, K., Hodges, K.V., 2001. Monazite–xenotime thermochronometry: methodology and an example from the Nepalese Himalaya. Contributions to Mineralogy and Petrology 141, 233–247.

Wu, C., Nelson, K.D., Wortman, G., Samson, S.D., Yue, Y., Li, J., Kidd, W.S.F., Edwards, M.A., 1998. Yadong cross structure and South Tibetan detachment in the east central Himalaya (89°–90°E). Tectonics 17, 28–45.

Zhu, B., Kidd, W.S.F., Rowley, D.B., Currie, B.S., Shafique, N., 2005. Age of initiation of the India–Asia collision in the east-central Himalaya. Journal of Geology 113, 265–285.